0026-895X/01/5905-996–1011$3.00
MOLECULAR PHARMACOLOGY
Copyright © 2001 The American Society for Pharmacology and Experimental Therapeutics
Mol Pharmacol 59:996–1011, 2001

Vol. 59, No. 5
501/896387
Printed in U.S.A.

Molecular Cloning, Genomic Positioning, Promoter Identification, and Characterization of the Novel Cyclic AMP-Specific Phosphodiesterase PDE4A10

GRAHAM RENA,[1] FIONA BEGG,[2] ANNETTE ROSS,[3] CAROLYNN MACKENZIE, IAN MCPHEE,[4] LACHLAN CAMPBELL, ELAINE HUSTON, MICHAEL SULLIVAN,[5] and MILES D. HOUSLAY

Molecular Pharmacology Group, Division of Biochemistry and Molecular Biology, Institute of Biomedical and Life Sciences, University of Glasgow, Glasgow, Scotland, United Kingdom

Received August 18, 2000; accepted January 12, 2001

This paper is available online at http://molpharm.aspetjournals.org

ABSTRACT

We describe the cloning and expression of HSPDE4A10, a novel long form splice variant of the human cAMP phosphodiesterase *PDE4A* gene. The 825 amino acid HSPDE4A10 contains a unique N terminus of 46 amino acids encoded by a unique 5′ exon. Exon-1^{4A10} lies ~11 kilobase pairs (kb) downstream of exon-1^{4A4} and ~13.5 kb upstream of the PDE4A common exon 2. We identify a rat PDE4A10 ortholog and reveal a murine ortholog by nucleotide sequence database searching. PDE4A10 transcripts were detected in various human cell lines and tissues. The 5′ sequence flanking exon-1^{4A10} exhibited promoter activity with the minimal functional promoter region being highly conserved in the corresponding mouse genomic sequence. Transient expression of the engineered human PDE4A10 open reading frame in COS7 cells allowed detection of a 121-kDa protein in both soluble and particulate fractions. PDE4A10 was localized primarily to the perinuclear region of COS7 cells. Soluble and particulate forms exhibited similar K_m values for cAMP hydrolysis (3–4 μM) and IC_{50} values for inhibition by rolipram (50 nM) but the V_{max} value of the soluble form was ~3-fold greater than that of the particulate form. At 55°C, soluble HSPDE4A10 was more thermostable ($T_{0.5}$ = 11 min) than the particulate enzyme ($T_{0.5}$ = 5 min). HSPDE4A10 and HSPDE4A4B are shown here to be similar in size and exhibit similar maximal activities but differ with respect to sensitivity to inhibition by rolipram, thermostability, interaction with the SRC homology 3 domain of LYN, an SRC family tyrosyl kinase, and subcellular localization. We suggest that the unique N-terminal regions of PDE4A isoforms confer distinct properties upon them.

cAMP serves as a key second messenger that is responsible for regulating many important cellular processes. Its levels are determined through the complex regulation of both its synthesis involving multienzyme families of adenylyl cyclase and its degradation by cAMP phosphodiesterases (PDE) (Houslay and Milligan, 1997). Indeed, a number of therapeutically useful agents have been designed to exploit differences in both the receptor subtypes that serve to regulate adenylyl cyclase activity and the activity of various PDE isoenzymes that are responsible for cAMP degradation. An additional regulatory feature is that various of the enzymes involved in cAMP signaling have also been shown to exhibit distinct intracellular localizations, leading to the phenomenon of compartmentalization of cAMP signaling in cells (Houslay and Milligan, 1997; Colledge and Scott, 1999).

Around eight different gene families encode PDEs that are able to hydrolyze cAMP (Beavo, 1995; Manganiello et al., 1995a,b; Houslay et al., 1998; Conti and Jin, 1999). The availability of selective inhibitors for several of these enzymes has demonstrated that certain PDEs have distinct roles in controlling the functioning of particular cellular processes. Indeed, recently, there has been considerable interest

This work was supported financially by the Medical Research Council (UK).

[1] Current address: MRC Protein Phosphorylation Unit, Department of Biochemistry, University of Dundee, Dundee DD1 5EH, Scotland.
[2] Current address: Grant Management, 20-23 Woodside Place, Glasgow G3 7QF, Scotland, UK.
[3] Current address: Department of Botany, University of Cambridge, Cambridge, CB12 1QW, England, UK.
[4] Current address: Scottish Biomedical, Block H, Ground Floor, Telford Pavilion, Todd Campus West of Scotland Science Park, Glasgow G20 0XA, Scotland, UK.
[5] Current address: AstraZeneca R&D Charnwood, Bakewell Road, Loughborough, Leicestershire, LE11 5RH, England, UK.

ABBREVIATIONS: PDE, cAMP phosphodiesterase; rolipram, 4-[3-(cyclopentoxyl)-4-methoxyphenyl]-2-pyrrolidone; UCR, upstream conserved region; PDE4, rolipram-inhibited, cAMP-specific phosphodiesterase; cDNA, complementary DNA; RT-PCR, reverse transcription-polymerase chain reaction; DTT, dithiothreitol; bp, base pair(s); kb, kilobase pair(s); ORF, open reading frame; DMEM, Dulbecco's modified Eagle's medium; IBMX, 3-isobutyl-1-methylxanthine; KHEM, KCl/ HEPES/EGTA/MgCl2; PAGE, polyacrylamide gel electrophoresis; TBS/Tween20, Tris-buffered saline/Tween 20; SH3 domain, SRC homology 3 domain; LYN, a SRC family tyrosyl kinase; GST, glutathione *S*-transferase; ATCC, American Type Culture Collection; HEK, human embryonic kidney; CREB, cAMP response element binding protein.

in the PDE4 cAMP-specific PDE family, as selective inhibitors of these enzymes, for which rolipram is the paradigm, having both anti-inflammatory and antidepressant properties (Bolger, 1994; Souness and Rao, 1997; Houslay et al., 1998; Rogers and Giembycz, 1998;Torphy, 1998). This has led to the development of PDE4-selective inhibitors for treatment of a variety of inflammatory disease states, with a particular focus on respiratory diseases such as asthma and chronic obstructive pulmonary disease (Torphy et al., 1999). Although PDE4-specific inhibitors seem to have considerable potential, various side effects, such as nausea, have been noted with some of these compounds, including, in particular, rolipram (Souness and Rao, 1997; Torphy, 1998). The molecular and cellular basis of such side effects is not known. However, the appreciation that a large family of PDE4 enzymes exists, suggests that an ability to target only certain of these isoforms may allow for the potentiation of therapeutic effects while minimizing side effects.

To date, more than 16 different PDE4, cAMP-specific isoforms have been identified (Houslay et al., 1998). Four separate genes (A, B, C, and D) encode these various isoforms, with the additional multiplicity being due to alternative messenger RNA splicing and the use of different promoters. Two conserved stretches of amino acids, called UCR1 and UCR2, provide unique characteristics of this enzyme family (Bolger et al., 1993; Bolger, 1994). These seem to interact and form a regulatory module (Beard et al., 2000) that is located between the isoform-specific N-terminal region and the catalytic unit. Two major classes of PDE4 isoforms, however, have been identified. These are the so-called "long" PDE4 isoforms, which possess both UCR1 and UCR2, and the short isoforms, which lack UCR1. The various PDE4 isoforms are then individually characterized by their unique N-terminal regions that, in a number of instances, have been shown to define the intracellular targeting of particular isoforms and to influence their catalytic activity (Shakur et al., 1993; Houslay et al., 1998; McPhee et al., 1999; Yarwood et al., 1999).

Three human PDE4A isoforms have been identified to date (Sullivan et al., 1998). Most interest has focused on the long HSPDE4A4B isoform (pde46; GenBank accession number L20965) and its rat homolog RNPDE4A5 (rdpe6; GenBank accession number L27057). These isoforms are widely expressed, being found in a variety of brain regions and cells associated with inflammatory responses (Livi et al., 1990; Bolger et al., 1993, 1994; McPhee et al., 1995; Seybold et al., 1998; MacKenzie et al., 2000). The RNPDE4A8 long form has, to date, only been characterized from rat and its expression seems to be restricted to testis (Bolger et al., 1996). Only one PDE4A short form has been identified, namely, PDE4A1, and the expression of this exclusively membrane-associated species is, seemingly, restricted to brain (Davis et al., 1989; Shakur et al., 1995). In addition, the curious HSPDE4A7 isoform (2el; GenBank accession number U18088), occurs as a catalytically inactive species due to two splicing events that cause both N- and C-terminal truncation of the enzyme catalytic region (Horton et al., 1995).

Recently we have identified (Sullivan et al., 1998) a 210-kb genomic contig for the human *PDE4A* gene locus. The *PDE4A* gene extends over about 50 kb and is orientated 5′-3′, telomere to centromere, at p13.2 on human chr19. This contig has allowed us to define the structure of the 15 exons that define the core UCR and catalytic regions of PDE4 enzymes. In addition, it has allowed for the identification (Sullivan et al., 1998) of the unique exons encoding the isoform-specific N-terminal regions of HSPDE4A1 and HSPDE4A4 as well as the putative HSPDE4A5 long form (TM3). Here we have used this contig as a resource to facilitate the molecular cloning of a novel human long PDE4A isoform, called HSPDE4A10 (GenBank accession number AF073745). To date, HSPDE4A4B has been the only PDE4A isoform known to be widely expressed and has thus provided the focus for analyzing the action of selective inhibitors. Our identification here of a novel, human PDE4A isoform with different intracellular distribution and sensitivity to the action of rolipram, compared with HSPDE4A4B, can be expected to have important consequences in trying to analyze and develop inhibitors selective for different PDE4 subfamilies.

Materials and Methods

Protease inhibitor tablets were obtained from Roche Molecular Biochemicals (Mannheim, Germany). [^{3}H]cAMP and enhanced chemiluminescence reagents were from Amersham Pharmacia Biotech (Little Chalfont, Buckinghamshire, UK). Dithiothreitol, Triton X-100, and *N*-[1-(2,3-dioleoyloxy)propyl]-*N*,*N*,*N*,-trimethylammonium methylsulfate were obtained from Boehringer-Mannheim. Bradford reagent was from Bio-Rad (Herts, UK). Rolipram was a kind gift from Schering (Berlin, Germany). All other materials were from Sigma (Poole, UK). DNA manipulation and sequence analysis were performed as described previously (Sullivan et al., 1998).

Isolation of PDE4A10, a Novel PDE4A cDNA. This was done as described previously (Huston et al., 1997). Briefly, we screened a rat olfactory lobe cDNA library (Stratagene, La Jolla, CA) using a probe reflecting the N-terminal half of UCR1, a region that is found in all PDE4 long forms. The probe was formed from nucleotides 1676 to 1877 of RNPDE4A5 (Bolger et al., 1994).

Isolation of RNA. RNA was isolated from tissue using Tri-Reagent (Sigma) (1 ml/50–100 mg of tissue) using a sterilized glass homogenizer (sample volume not to exceed 10% of the volume of Tri-Reagent used). Adherent cell monolayers were scraped into Tri-Reagent (1 ml) and resuspended with a pipette. Cells grown in suspension were lysed by addition of Tri-Reagent to pelleted cells and resuspended with a pipette. Tri-Reagent fractionation was performed according to the manufacturer's instructions. Briefly, the homogenate was stored at room temperature for 5 min. Cell membranes, polysaccharides, and high molecular weight DNA were then pelleted by centrifugation at 12,000*g* for 10 min at 4°C. The supernatant was taken and RNA and DNA were phase separated by addition of 0.2 ml of RNase-free chloroform per 1 ml of Tri-Reagent. The solution was vortexed for 15 s and then stored at room temperature for 3 min. Phase partition was brought about by centrifugation at 12,000*g* for 15 min at 4°C. For RNA isolation the aqueous phase was taken and the RNA precipitated by addition of isopropanol (propan-2-ol): 0.5 ml/1 ml of Tri-Reagent used initially. Precipitation was allowed to continue for 5 to 10 min at room temperature. RNA was then pelleted by centrifugation at 12,000*g* for 10 min at 4°C and taken up in 1 ml of 75% ethanol and stored at −80°C. It was then prepared for use by centrifugation at 7500*g* for 5 min at 4°C, the supernatant aspirated and the RNA pellet dried under vacuum. RNA was resolubilized in di-ethyl pyrocarbonate-treated water.

Reverse Transcription-Polymerase Chain Reaction (RT-PCR). Reverse transcription was performed by kit (Amersham Pharmacia Biotech), as directed by the kit protocol. Briefly, 5 μg of total RNA in H_2O (20 μl) was heated to 65°C in a thermal cycler for 10 min and then immediately chilled on ice. The "Bulk first-strand cDNA mix" was gently suspended and then collected by centrifugation. The cDNA synthesis reaction was prepared on ice and contained 11 μl of

Bulk first-strand cDNA mix, 1 μl of DTT solution, 40 pmol of primer, and 20 μl of heat-denatured RNA. The cDNA synthesis reaction was incubated at 37°C for 1 h.

Amplification of PDE4A10-specific fragments from rat and mouse cDNA was carried out using the primer pair GR10 and GR11, designed to amplify an 86-bp fragment. The sense primer GR10 (Table 1) binds to the extreme 5′ end of the partial rat PDE4A10 cDNA (GenBank accession number AF110461), whereas the 3′ primer GR11 (Table 1) is complementary to the upper strand and binds toward the 3′ end of the unique sequence that is found at the 5′ end of the rat PDE4A10 cDNA. A 220-bp human PDE4A10-specific fragment was amplified from cDNA derived from cell lines using the primer pair GR10 and GR84. The 3′ primer GR84 (Table 1) is complementary to the upper strand and binds sequence derived from exon-2. To monitor human tissue expression of the PDE4A10 mRNA a Human Rapid-Scan Panel (OriGene Technologies, Rockville, MD) containing cDNA prepared from 24 human tissues was used according to the manufacturer's instructions as templates in a PCR reaction containing the sense primer MS-FB11 and the antisense primer MS-FB12 (Table 1). The PCR product (247 bp) was characterized by subcloning into pCRII (Invitrogen, San Diego, CA) and sequence analysis. To probe human "panel 1" RNA (CLONTECH, Palo Alto, CA) the sense primer IM1 (Table 1) was used together with the antisense primer IM2 (Table 2) to amplify a 313-bp fragment. In each case RNA was normalized for β-actin.

Generation of Human PDE4A10 Expression Plasmids. The ORF encoding the 825 amino acids of human PDE4A10, as predicted from the HSPDE4A genomic sequence and cDNA fragments, was engineered for expression. A 526-bp *Sau*3AI fragment from clone 67 (see below) containing 399 bp of 5′-untranslated sequence, the start codon of the HSPDE4A10 ORF, and all but the last 6 bp of exon-1^{4A10}, the unique 5′ exon for the long PDE4A10 isoform (GenBank accession numbers AF178570 & AF295325), was ligated to unphosphorylated adapters (upper strand 5′-gatcTGTCAGCTTCGAa-3′ and lower strand 5′-TCGAAGCTGACA-3′). These adapters anneal to form a Sau3A-I sticky end, contain a BstBI site (underlined), and a single adenine residue overhang. The adapters also contain the six bases from the 3′ end of the HSPDE4A10 5′-exon that are missing from clone 67 and the first six bases of the HSPDE4A common exon-2 (in uppercase text in the upper strand oligonucleotide as shown above). After ligation of the annealed adapters to the Sau3A-I fragment this DNA was then cloned into the pCR2.1 TA cloning vector (Invitrogen, Carlsbad, CA). A clone with the insert in the desired orientation was completely digested with *Kpn*I and then partially digested with BstBI to release a 607-bp fragment. The *Kpn*I/*Bst*BI fragment was ligated with pSV-SPORT-pde46 that had been digested first with *Kpn*I and then partially digested with *Taq*I to release the sequence that encodes the unique N terminus of HSPDE4A4B and the first three bases of the common exon-2 sequence. Replacing the released HSPDE4A4B fragment with the HSPDE4A10 *Kpn*I/BstBI fragment generated pSV-SPORT4A10 and contained the complete HSPDE4A10 ORF. Although pSV-SPORT4A10 contains the complete HSPDE4A10 ORF it also contains 399 bp of untranslated sequence upstream of the HSPDE4A10 start codon and includes an upstream out of frame ATG. To ensure optimal expression of the HSPDE4A10 ORF the 5′-untranslated region containing the upstream ATG was removed. The region encoding the N-terminal 442 amino acids of HSPDE4A10 was amplified by PCR using pSV-SPORT4A10 as template with primers FB4A10f2 and 4A10FB22R. Oligonucleotide FB4A10f2 (5′-CGACggtaccGGCTACCATGCGCTCCGGTGCAGC-3′) binds at the extreme 5′ end of the PDE4A10 ORF and contains an upstream *Kpn*I restriction site (in lowercase text shown above). The 3′ primer 4A10FB22R (5′-TCGAGCACCGACTCATCGTTGTAC-3′) is complementary to the upper strand and binds at the internal *Xho*I restriction site (underlined above) in the PDE4A ORF. The PCR was done using the Expand High Fidelity PCR System (Roche Molecular Biochemicals). The PCR product was cloned into pCR2.1 TA cloning vector and clones were sequenced to select one that contained no base changes that would lead to altered amino acids encoded by the HSPDE4A10 ORF. The 1333-bp *Kpn*I/*Xho*I fragment was removed from the pCR2.1 TA vector and used to replace the 1785bp *Kpn*I/*Xho*I fragment from pSV-SPORT4A10 to generate pSV-SPORT4A10f2 that lacks the large 5′ untranslated region, including the upstream out-of-frame ATG.

Isolation and Sequencing of a Subclone Containing Exon-1^{4A10}. Cosmid 29158 was digested with *Xho*II to obtain a library of subclones of the cosmid. After treatment with *Taq* polymerase, the resulting fragments were cloned into the pCR2.1 TA cloning vector (Invitrogen). A PCR screen of this library identified a 2.5-kb clone (clone 67) containing the putative exon-1^{4A10}. Clone 67 was subjected to complete digestion with *Hga*I, which cuts away from its recognition site to give unique ends. These ends were then used (Rena and Houslay, 1998) to identify which digestion fragments are contiguous in the original clone. Such fragments are ostensibly uncloneable because the cohesive end can have any sequence. However, this problem can be solved (Rena and Houslay, 1998) by filling in the ends of the digestion fragments with *Taq* Polymerase followed by TA cloning. The four different fragments obtained were assembled into a contig simply by inspection of their end sequences, as discussed in detail previously by us (Rena and Houslay, 1998). This novel sequencing method (Rena and Houslay, 1998) was used to identify rapidly the position of the human PDE4A10 exon in a 2.5-kb subclone of a cosmid containing genomic DNA and the presumed PDE4A10 exon as implicated by PCR. Simple "primer walking" sequencing of this fragment proved to be problematic due to its extremely high GC content. To obviate this we adopted the new methodology. Importantly, however, we confirmed the positioning of the PDE4A10 exon by sequencing partial digests of the 2.5-kb fragment and PCR of the 2.5-kb fragment as previously described (Rena and Houslay, 1998). Direct sequencing of cosmid 32166 identified the final 6 bp of exon-1^{4A10} and its 3′ intron flanking sequence.

Deletion Mutagenesis and Point Mutations. Site-directed mutagenesis was performed using a QuickChange DNA mutagenesis kit (Stratagene Ltd., Cambridge, UK) according to the manufacturer's instructions. The Δb-PDE4A10 deletion mutant was generated by site-directed mutagenesis using the QuickChange Mutagenesis system according to the manufacturer's instructions. This mutant was analogous to the Δb-PDE4A4B deletion mutant described before by us (McPhee et al., 1999) and was formed by the removal of amino acids 252–260 (APRPRPSQ), within the LR2 region of PDE4A10. All mutagenesis and deletion constructs were confirmed by DNA sequencing.

TABLE 1

Primer pairs used

The positions of the primers are shown schematically in Fig. 1. For the GR primer set, GR29 (CAGGGTGRTCCACATCGTGG) was used to prime PDE4A specific first-strand cDNA synthesis. For the others (IM and MS-FB sets), the PDE4A-specific primer used was ESH4 (TGGTGATTCTCGAGCACCGAC). GR10/GR84 are used in the same way as IM1 and IM2. Both primer pairs were validated against positive and negative controls and amplification products were cloned and sequenced to confirm specificity. The IM1/IM2 pair used PCR conditions of 95°C for 5 min, 40 cycles of 94°C for 30 s, 60°C for 30 s, 72°C for 1 min, 72°C for 10 min, and then 4°C before use. The MS-FB11/MS-FB12 pair utilized PCR conditions of 35 cycles; 94°C for 30 s, 55°C for 30 s, and 72°C for 1 min.

Primer	Sequence (5′–3′)	Band Size
GR10	GCATTGCCCCTAGGACCAGAGTC	90
GR11	CAAGCTGACACATCTGCCCGGAG	
GR114	GCAGGACCCCTGCAGG	365
GR11	CAAGCTGACACATCTGCCCGGAG	
GR10	GCATTGCCCCTAGGACCAGAGTC	224
GR84	TCGCTGTCTGAGCGGTACAGGAAG	
IM1	TCCGGGCAGATCTGTCAGCTT	313
IM2	ACTGGGAACGGGCACATTGGT	
MS-FB11	CCGGGCAGATCTGTCAG	247
MS-FB12	CCTGAGCAAATGGTGTTACG	

Cell Culture and Transfection. COS7 cells were maintained and transfected essentially as described previously by us (Huston et al., 1996). COS7 cells were seeded at approximately 33% confluence onto 10-cm-diameter plates. Immediately before transfection, the culture medium was replaced with 5 ml of Dulbecco's modified Eagle's medium (DMEM) supplemented with 10% (v/v) newborn calf serum together with 0.1 mM chloroquine. DNA (10 μg) was diluted to 250 μl with Tris/EDTA buffer (10 mM Tris, 0.1 mM EDTA, pH 7.6) and 200 μl of 10 mg/ml DEAE dextran was then added. The mixture was incubated at room temperature for 15 min before addition to the culture medium. Cells were incubated at 37°C, 5% CO_2 for 3 to 4 h before the medium was aspirated and the cells shocked for 2 min with 10% dimethyl sulfoxide in a PBS solution. The culture was then rinsed twice in PBS solution before DMEM containing 10% fetal calf serum was added, and the cells were incubated at 37°C in a 5% CO_2 atmosphere for 72 h. The human glioblastoma cell lines U-118 MG [American Type Culture Collection (ATCC) HTB-15] and U-87 MG (ATCC HTB-14), the SK-N-SH human neuroblastoma cell line and the HeLa S3 human cervical carcinoma cell line (ATCC CCL-2.2) were all passaged 1:5 every other day while grown in DMEM (Sigma) supplemented with penicillin/streptomycin (100 U/ml; Sigma), 10 mM glutamine (Sigma), and 10% fetal calf serum (Sigma). U-937 human monocyte-like lymphoma cells (ATCC CRL-1593.2) and Jurkat J6 human leukemic T cells were grown as a suspension in continuous culture using the same medium as described above. The human follicular thyroid carcinoma cell lines FTC133 cell line was cultured in RPMI medium (Sigma).

Subcellular Fractionation of COS7 Cells. Disruption of cells and the isolation of particulate and high-speed supernatant fractions were done as described in detail previously (Huston et al., 1996). Fractionation was carried out in KHEM buffer (50 mM KCl, 50 mM HEPES, final pH 7.2, 10 mM EGTA, 1.92 mM $MgCl_2$) containing protease inhibitors. In some experiments, as indicated in the text, various (final) concentrations the nonionic detergent Triton X-100 were added to PDE assays that contained 2 μg of protein from the indicated subcellular fractions.

Luciferase Plasmid Constructs. A 1.8-kb *Nco*I/*Eco*RI fragment containing exon-1^{4A10} and both 5′ and 3′ flanking sequences was blunt-ended using Klenow polymerase and cloned into the *Sma*I site of pGL3-Basic (Promega, Madison, WI) to generate pFL-Luc. Using pFL-Luc a series of 5′ deletions containing smaller fragments of the exon-1^{4A10} 5′ flanking region were constructed. In short, 10 μg of *Mlu*I/*Kpn*I-digested pFL-Luc was purified and incubated with exonuclease III at a final concentration of 150 units/pmol. DNA samples were removed from the reaction at 30-s intervals and incubated with SI nuclease. Pools of samples were then blunt-ended using Klenow polymerase and self-ligated. Plasmid DNA isolated from transformed colonies was digested with *Bam*HI to check for insert size and selected plasmids were then sequenced. Four deletion plasmids; Δ1, Δ2, Δ3, and Δ4 were used in comparison with pFL-Luc to determine promoter activity of the human exon-1^{4A10} 5′ flanking region.

Transfection and Detection of Luciferase Activity. HEK293 cells were transfected using the *N*-[1-(2,3-dioleoyloxy)propyl]-*N*,*N*,*N*,-trimethylammonium methylsulfate method (Roche Molecular Biochemicals). After transfection the Dual-Luciferase reporter assay system (Promega) was used to measure both firefly and Renilla luciferase activity. Ten micrograms of each firefly luciferase construct was cotransfected with 100 ng of the control Renilla luciferase construct (pRL-CMV; Promega). After 48 h cells were harvested and washed twice in PBS and lysed with 600 μl of 1× passive lysis buffer (Promega). After determination of the protein concentration, 10 to 50 μg of protein was assayed; first for firefly luciferase activity, and then, after quenching and initiation of the Renilla luciferase reaction, the Renilla activity was measured according to the manufacturer's instructions on a MLX Microtitre Plate Luminometer (Thermo Labsystems, Helsinki, Finland). Substrate (100 μl) was added, as per the manufacturer's instructions, and the scale set to autogain with a 2-s integration followed by a 10-s read time. Luciferase activity was expressed as relative light units. The measured firefly luciferase activity for each of the human PDE4A10 promoter constructs was divided by the measured control Renilla luciferase activity for each transfection and then normalized with respect to the activity measured for pFL-Luc, which was set as 1. In some experiments analyses were done after 0.5, 4, 16, and 24 h using HEK293 cells that had been incubated with either IBMX (100 μM), forskolin (100 μg/ml), or IBMX + forskolin, phorbol-12-myristate-13-acetate (100 or 500 nM), or epidermal growth factor (50 ng/ml).

Computer Analysis of the PDE4A10 5′ Intronic Sequence. The 1.34 kb of genomic 5′ flanking sequence lying between the last base of exon-1^{TM3} and the start codon of the human exon-1^{4A10} was analyzed by PROSCAN (version 1.7), a Pol II promoter prediction program (Prestridge, 1995). The mouse and human sequences upstream of exon-1^{4A10} were compared with each other using the BLAST 2 algorithm to identify conserved regions.

SDS-PAGE and Western Blotting. Acrylamide gels (8%) were used and the samples boiled for 5 min after being resuspended in Laemmli buffer. Gels were run at 8 mA/gel overnight or 50 mA/gel for 4 to 5 h with cooling. For detection of transfected PDE by Western blotting, 2- to 50-μg protein samples were separated by SDS-PAGE and then transferred to nitrocellulose before being immunoblotted using specific antisera. Labeled bands were identified by using anti-rabbit peroxidase-linked IgG and the Amersham enhanced chemiluminescence Western blotting was used as a visualization protocol. The human PDE4A antiserum used in this study has been described in detail previously by us (Huston et al., 1996). This antiserum was generated to detect specifically the unique C-terminal region found in common to all catalytically active human PDE4A isoforms.

ELISA Detection of PDE4A Isoforms. This was done essentially as we have described before in some detail (Huston et al., 1996). The bait protein was diluted in carbonate buffer pH 9.6 (C-3041; Sigma) over a range of concentrations in a final volume of 100 μl and plated out in triplicate on a 96-well ELISA plate and incubated overnight at 4°C. The plate was then washed three times with Tris-buffered saline pH 7.4, containing 0.05% Tween 20 (TBS/Tween20) before blocking in 1% milk powder for 2 h at room temperature. After three washes in TBS/Tween20, plates were incubated

TABLE 2

Properties of PDE4A10 expressed in COS cells

COS7 cells were transfected to express PDE4A10 transiently before subcellular fractionation into high-speed supernatant (S2), high-speed pellet (P2), and low-speed pellet (fractions). The distribution of PDE4A10 in these fractions was ascertained by quantitative immunoblotting. The IC_{50} value for rolipram inhibition in each case was determined using 1 μM cAMP as substrate. K_m and V_{max} values were determined by kinetic analysis, as described under *Materials and Methods.* To allow comparison between PDE4A10 expressed in the various fractions, we show here the relative V_{max} values compared with PDE4A10 in the S2 fraction (given here as unity). COS7 cells were also transfected so as to express PDE4A4B and its distribution was ascertained in these fractions by quantitative immunoblotting. Data given in parentheses are for the distribution of PDE4A4B reported previously (McPhee et al., 1999). These data are given as means ± S.D. for three separate cell transfection experiments, except for distribution data for PDE4A10, where $n = 6$.

K_m	Fraction	IC_{50} Rolipram	Relative V_{max}	Distribution 4A10	Distribution 4A4B
μM		nM		%	%
2.9 ± 0.6	S2	56 ± 6	(1)	83 ± 7	58 ± 7 (55)
3.8 ± 1.1	P2	52 ± 8	0.31 ± 0.03	10 ± 7	24 ± 6 (26)
4.1 ± 0.5	P1	54 ± 8	0.48 ± 0.05	7 ± 4	18 ± 6 (19)

for 2 h at room temperature with primary antibody (1/1000) dilution in TBS containing 0.1% milk powder. Plates were washed again in TBS/Tween20 and incubated with secondary antibody conjugated to alkaline phosphatase (1/30,000 dilution) in 1% milk powder for 1 h at room temperature. A further six washes in TBS/Tween20 were followed by the addition of 100 μl of substrate (4-nitrophenolphosphate) at a concentration of 1 mg/ml in a buffer of 0.1 M glycine, 0.001 M zinc chloride, and 0.001 M magnesium chloride, pH 10.4. After 30- to 60-min incubation in the dark, the absorbance at a wavelength of 405 nm was read on a multiplate reader.

PDE Assay. Cyclic nucleotide phosphodiesterase activity was assayed by a modification of the two-step procedure of Thompson and Appleman (1971) as previously described by us (Marchmont and Houslay, 1980). All assays were conducted at 30°C and in all experiments a freshly prepared slurry of Dowex/H_2O/ethanol (1:1:1) was used for determination of activities. Initial rates were taken from linear time courses of activity. All kinetics measurements were performed as previously described by us (Huston et al., 1996). To define K_m and V_{max} values, PDE assays were done over a range of cAMP substrate concentrations. These were then analyzed as before (Huston et al., 1996) by computer fitting to the hyperbolic form of the Michaelis-Menten equation using an iterative least-squares procedure (Ultrafit; with Marquardt algorithm, robust fit, experimental errors supplied; Biosoft, Cambridge, UK). As described before in some detail (Bolger et al., 1994; McPhee et al., 1995, 1999), relative V_{max} values were obtained by using equal amounts of PDE4A immunoreactive protein in assays as determined using the PDE4A-specific C-terminal antiserum. In mixing experiments, 2 μg of protein from the P2 and S2 fractions were assayed both separately and together. Total PDE4 activity in cells was determined at a substrate concentration of 1 μM cAMP and defined as that amount of PDE activity that could be inhibited by the addition of 10 μM rolipram. This is a concentration at which rolipram serves as a PDE4-selective inhibitor and can completely inhibit PDE4 activity (Houslay et al., 1998).

Thermostability Analyses. This was done as we described previously (Marchmont and Houslay, 1980). Briefly, 200-μl samples of 20 mM Tris-HCl buffer pH7.4 were prewarmed to 55°C in a Microfuge tube before the addition of a 5-μl aliquot from either the cytosol or the P1 or the P2 fraction from COS7 cells that had been transfected to express either PDE4A10 or PDE4A4B. At the indicated time, a 50-μl sample was removed into an ice-cold Microfuge tube before being taken for PDE assay. These samples contained approximately 4 μg/ml protein in each instance.

Confocal Analyses and Digital Deconvolution. COS7 cells were plated out onto coverslips (18 × 18 mm) at about 40% confluence 48 h after transfection. After another 24 h the cells were fixed for 30 min in 4% paraformaldehyde in TBS. Fixed cells were permeabilized with three changes of 0.2% Triton in TBS for 15 min. They were then subjected to four 5-min blocking incubations with 20% goat serum and 4% bovine serum albumin before being labeled for 2 h with polyclonal antibodies raised against specific peptide sequences of the C-terminal region common to all full-length PDE4A isoforms (Huston et al., 1996). Labeling was detected using either a fluorescein isothiocyanate- or tetramethylrhodamine isothiocyanate-conjugated goat anti-rabbit IgG for 1 h. Localization of proteins was visualized using the complementary fluorescein isothiocyanate- or tetramethylrhodamine isothiocyanate-conjugated goat anti-mouse IgG to the polyclonal staining. All incubations were carried out at room temperature. Cells were visualized using a laser-scanning confocal microscope using an Axiovert 100 microscope (Carl Zeiss, Welwyn Garden City, UK) with a X63/1.4NA plan apochromat lens, as described previously (Huston et al., 1996).

Pull-Down Assays with LYN-SH3. This was done essentially as described before by us in some detail (O'Connell et al., 1996; McPhee et al., 1999). Briefly, volumes of slurry containing 400 mg of the fusion protein immobilized on glutathione agarose beads were pelleted and the supernatants discarded. Within each assay, volumes taken were equalized with washed beads. The pellets were resuspended in the cytosol from COS7 cells that had been transiently transfected to express the indicated PDE4A form. To allow for the binding of PDE4A4 and PDE4A10 to LYN-SH3 to be compared, and then, as described previously by us (Huston et al., 1996), an amount of cytosol fraction containing equal amounts of these enzymes, as assessed immunologically, was taken. The amount of PDE4A4B was chosen such that about 40 to 50% became bound to LYN-SH3; this was usually of the order of 100 mg of protein. These were diluted to a final volume of 200 μl in KHEM buffer containing 1 mM DTT and protease inhibitor cocktail. The immobilized fusion protein and cytosol were incubated together for 10 min end-over-end at 4°C. The beads were then collected by centrifugation for 5 s at high speed in a benchtop centrifuge and the supernatant retained as the unbound fraction. The beads were held on ice and washed three times with 400 μl of KHEM containing 1 mM DTT and protease inhibitor cocktail over a 15-min period. These washes were pooled along with the unbound fraction and aliquots taken for Western blotting along with fraction of the bound PDE.

Results

Except where indicated, all results are presented in triplicate or are representative of results found in at least three separate experiments.

Identification of a Rat PDE4A10 Partial cDNA. Long PDE4 isoforms are characterized (Houslay et al., 1998) by two conserved blocks of sequence called UCR1 and UCR2 (Fig. 1). Screening of a rat olfactory lobe cDNA library with a probe against a portion of UCR1 allowed for the identification of a cDNA clone whose sequence (data not shown) identified it as forming part of a novel rat PDE4A long form that we call here RNPDE4A10 (GenBank accession number AF110461). The sequence of the 3′ portion was identical to that of the established rat PDE4A long isoforms, RNPDE4A5 (rpde6) (Bolger et al., 1994) and RNPDE4A8 (rpde39) (Bolger et al., 1996) and encompassed the entire C-terminal and catalytic regions together with both UCR1 and UCR2 (Bolger et al., 1994; Houslay et al., 1998). The RNPDE4A10 cDNA contained 88 bases of novel sequence (Fig. 2a) at the extreme 5′ end upstream of the common exon-2 sequence found in all long PDE4A isoform cDNAs (Bolger et al., 1996; Houslay et al., 1998). Transcripts for this novel isoform were successfully detected (Fig. 3a) using RNPDE4A10-specific primers

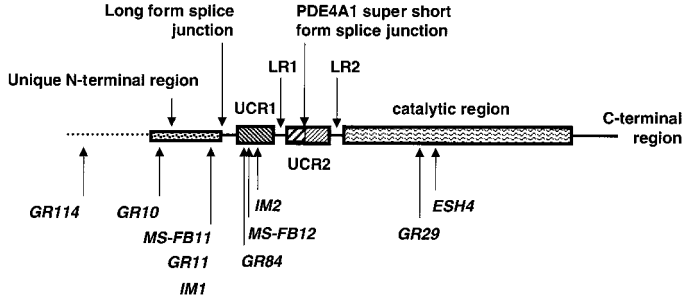

Fig. 1. Schematic diagram showing key features of long PDE4A isoforms. This diagram shows schematically the key regions that characterize PDE4 long isoforms. These are an N-terminal (5′) region that is unique to each isoform and that is encoded by an upstream 5′ exon; the upstream conserved regions UCR1 and UCR2; the linker regions LR1 and LR2 that join UCR1 to UCR2 and UCR2 to the catalytic unit, respectively; the catalytic region, and the C-terminal region. There are two known splice junctions that generate transcripts encoding active enzymes from the PDE4A gene. These are the super short PDE4A1 isoform junction that is located within UCR2 and the long form junction that is located upstream of UCR1. Also indicated are the positions of the various primers used in this study and whose sequence is given under *Materials and Methods*.

a

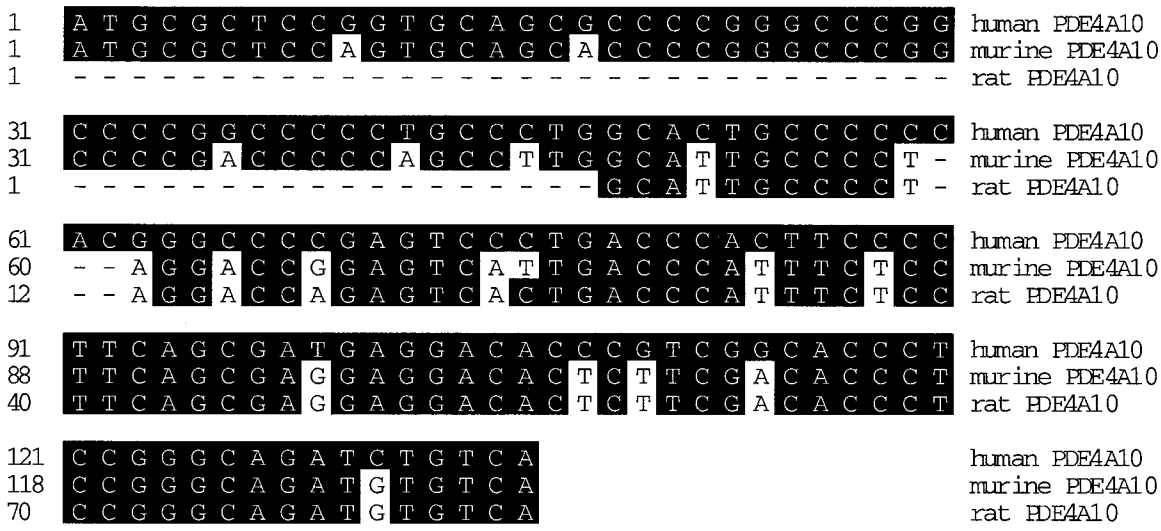

b

c

```
gtaagtgcagcgctggtggccgtgggttcaagtcgcccctggccacctggcgcactccagggtctagggttcgtggctcactctctccagc
ctcactttcctcttctgtcacatagcagcgatcaaaatcatccctgaccgccagggttgccctggagacctctgatagggcatgcagtaga
cgtttaataaatgttgcatccttcccacttcctgtgcaaacctgaagctgcggtcacgctttggaggagtgagggcgacctgccatccagg
tcatgtgttcatcctggggtatgtgttcagttctgtcagcctcagtctactggcctgtgaaatggggccagtcatgccttctgtgggtggc
cttgcggtgaggcttggtgtcactcctagtaccgggccacagagggcaaatggaagttccctttctggccagacggggtgggctgcggggg
cttgaagtctgggagtgacaggccccgaggccacatccagtctggctttctaatgtccttatatcctggaggcagaagttggcagcccgga
gttgggcactggctggccctgggggcttctccgggtcctcagcctcccccttccacctactttccacgtgcaattgaggcacagactga
aggagggcacggcggggcaggaccgggcccagcgactggccccaggaacgaaatggggcggggacagaagaggaagaggggccagggcctt
tgggagccccgcgtggggtccgcagggtgtgtgtagggaaatcgttgcttctctccgggtctctctctctgcgtcctgcgtctctgtctcc
acttctgtctcttctgtctctgttttgtttctccttcccaccgctgagctgcaccttcccctccctgggtttatgtcacccggccccaca
ctcgagtcccgtttccccgggggcgcacggcgatcagcgatcagagacctcgagcgggcccagctcgacgtcagggcggggaggggggaaa
ggcggggccggaggcggtggcaggagggcgggcccggagccgggaaACCGGAGCCCCGGGGCACCCCAGAGGCCTAGGAGGGAGGAGACGG
GGGGGGGGGGGGGAAGTGTGCTCCGACTCCGCAGGACCCCTGCAGGGGGAGGCAGACAGAGCGCCCGTGCGCTCCCCTCCCCCGTGCAGAC
CCGGGAACGCTCGACCGCCCGGGGCTGTCCCTGGGGGGGTCACCAGAGGCGTGGAGGCGGTGCCGGCAGTGGAGGCCGCAGACACCTTGGG
```

Exon 1-4A10

```
                                                                    MetArgSerGlyAlaAla
CCTGGCCAGCAGCGCGCGCCACACCGCCCTGCCGCCGTCCCCATGCGCGCCCCGACGACGGCGCTTGGCTCCCATGCGCTCCGGTGCAGCG
ProArgAlaArgProArgProProAlaLeuAlaLeuProProThrGlyProGluSerLeuThrHisPheProPheSerAspGluAspThrA
CCCCGGGCCCGGCCCCGGCCCCCTGCCCTGGCACTGCCCCCCACGGGCCCCGAGTCCCTGACCCACTTCCCCTTCAGCGATGAGGACACCC
rgArgHisProProGlyArgSerValSe                                    rPheGluAlaGluAsnGlyProThrPr
GTCGGCACCCTCCGGGCAGATCTGTCAGgtggggtggcc.....13.5kb.....cccatcccctgcagCTTCGAGGCAGAGAATGGGCCGACACC
```

Exon 2

```
oSerProGlyArgSerProLeuAspSerGlnAlaSerProGlyLeuValLeuHisAlaGlyAl
ATCTCCTGGCCGCAGCCCCCTGGACTCGCAGGCGAGCCCAGGACTCGTGCTGCACGCCGGGGC
```

Fig. 2. Unique N-terminal region of the long PDE4A isoform, PDE4A10 and the human exon-1^{4A10} genomic sequence. a, novel 5′ sequence for the PDE4A10 isoform. Complete nucleotide sequence is shown from the initiating ATG for the human form (HSPDE4A10) aligned with both that of the rat form (RNPDE4A10), which is incomplete at the 5′ end, and the murine form (MUPDE4A10), which represents the 5′ end of the previously unassigned mouse EST cDNA (GenBank accession number BE531640). Conserved residues are shown in black boxes. Downstream sequence from that shown in this figure was 100% identical in the partial rat PDE4A10 cDNA clone (GenBank accession number AF110461) and the established full-length rat PDE4A long isoform cDNAs for PDE4A5 (rpde6) (GenBank accession number L27057) and PDE4A8 (rpde39) (GenBank accession number L36467). This common sequence begins as GCTTGGAGGCAGAAAAT and continues identically thereafter in these rodent forms. b, alignment of the conserved predicted N-terminal region of human, mouse, and rat PDE4A10. Conserved amino acids are in uppercase, whereas amino acids in the human sequence shown in bold text are not conserved in rat and mouse. In the rat sequence unknown amino acids are marked by X, as the rat cDNA clone (GenBank accession number AF110461) is a partial clone. c, human genomic sequence of the PDE4A10 5′ exon, exon-1^{4A10}, with 5′ and 3′ flanking nucleotides (GenBank accession number AF178570) and the start of the PDE4A long isoform common exon-2 is shown. Exon-1^{4A10} and exon-2 nucleotides are shown in uppercase letters and are labeled above the encoded amino acids; introns are in lowercase letters. The ORF of PDE4A10 is translated and the corresponding amino acids are shown in italics above the nucleotide sequence. The unique N-terminal amino acids encoded by PDE4A10 are shown in bold above the corresponding nucleotide sequence. The 5′ start of exon-1^{4A10} in the human sequence represents the equivalent adenine residue that represents the 5′ end of the previously unassigned mouse EST cDNA (GenBank accession number BE531640). The upstream out-of-frame ATG in exon 1^{4A10} that is conserved in human and mouse is underlined.

(Table 1) to amplify a fragment of the correct size from both rat olfactory lobe RNA and from mouse brain RNA. The 88 bases of novel sequence encode part of the unique N-terminal region of a novel isoform, RNPDE4A10 (Fig. 2a).

Initially, to determine whether the PDE4A10 isoform is conserved in humans, we used the rat sense PDE4A10-specific primer GR10, together with the antisense primer GR84, designed to sequence found in the common UCR1 region of long human PDE4A isoforms (Fig. 1) in RT-PCR analyses of human cell lines (Fig. 3b). A product of the expected size (220 bp) was amplified from the human U-118 (glioblastoma), SK-N-SH (brain), FTC133 (thyroid), and HEK293 (kidney) cell lines but not from either human U-87 (glioblastoma) or Jurkat T-cell lines (Fig. 3b). Sequence analysis of these PCR products revealed that the human sequence exhibited a high degree of homology with the novel sequence found at the 5′ end of RNPDE4A10 (data not shown). It also contained downstream "common" region (Figs. 1 and 2c) sequence derived from human PDE4A exon-2, indicating that the PDE4A10 isoform is conserved in human and rat. This pattern of domain "swaps" is regularly seen in PDE4 cDNAs with the divergence occurring upstream of the common exon-2 (Houslay et al., 1998) (Fig. 4).

Isolation and Characterization of the Human PDE4A10 5′ Exon (Exon-1^{4A10}). The rat PDE4A10 cDNA was not full length because it lacked an in-frame start codon. Using a variety of rapid amplification of cDNA ends (RACE) methods we were unable to determine the full extent of the 5′ end of this cDNA. We were to find out from subsequent analyses of human PDE4A10 that this was undoubtedly caused by the high GC content of the extreme 5′ region of PDE4A10. However, we took advantage of our recent mapping (Sullivan et al. 1998) of a 210-kb cosmid contig containing the human *PDE4A* gene to isolate, map, and fully characterize exon-1^{4A10}, encoding the N-terminal region that is unique to human PDE4A10.

To identify cosmids containing the HSPDE4A10-specific 5′ exon we used oligonucleotides GR10 and GR11 as a primer pair in a PCR screen using candidate cosmids as template DNA. This screen readily identified cosmids in the contig that contained exon-1^{4A10}, namely, cosmids 29158, 27270, 31069, and 32166 (Fig. 3c). These cosmids are found (Fig. 4a) at the 5′ end of the contig containing the PDE4A gene and have been shown previously to contain the 5′ exons encoding the unique N-terminal regions of the long PDE4A4 isoform (exon-1^{4A4}) and putative long isoform TM3 (exon-1^{TM3}) (Sullivan et al., 1998). As described under *Materials and Methods*, cosmid 29158 DNA was digested with *Xho*II to generate a library of subclones. A PCR screen of this library identified a 2.5-kb clone (clone 67) that was positive for the presence of

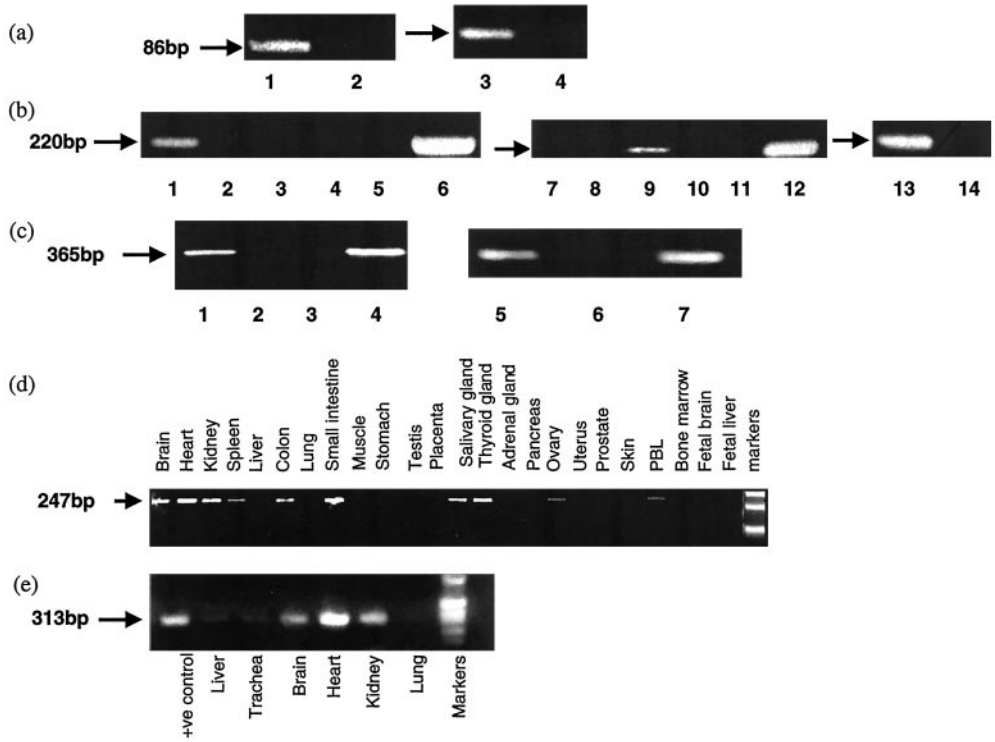

Fig. 3. PCR analysis for the unique 5′ end of PDE4A10 and tissue distribution of PDE4A10 in human tissues. a, primer pair GR10 and GR11 was designed to the ends of the unique rat PDE4A10 cDNA 5′ end sequence to amplify an 86-bp fragment as indicated. Products were sequenced to verify authenticity. This shows RT-PCR done on rat olfactory lobe RNA (track 1) and mouse brain RNA (track 3) with control lanes having no cDNA (tracks 2 and 4). b, these experiments used the sense primer GR10, designed to the 5′ end of the unique PDE4A10 sequence, and the antisense primer GR84, designed to amplify within the common region at the UCR1 border to detect a band of 220 bp. Products were sequenced to verify authenticity. Analyses were done on RNA from various human cell lines, HEK/293 (track 1), U87 (track 3), SK-N-SH (track 6), Jurkat (track 7), FTC133 (track 9), U118 (track 12), and HeLa (track 13). Control lanes are also shown (tracks 2, 4, 5, 8, 10, 11, and 14) for each of the various preparations. c, PCR done using GR11 with the upstream primer GR114 targeted within the unique PDE4A10 5′ intron and designed to amplify a 365-bp fragment. This was done on cosmid 27270 (track 1), cosmid 29158 (track 4), cosmid 32166 (track 5), and cosmid 31069 (track 7) and with negative controls in tracks 2, 3, and 6. d, human rapid-scan panel was analyzed by PCR, using the primer pair MS-FB11/MS-FB12, to monitor expression of PDE4A10 across a variety of human tissues (labeled above each lane). e, RT-PCR done on RNA from a variety of human tissues using the IM1 and ESH4 primers to amplify a 313-bp product. This analyzed a positive control (track 1) and negative control (track 9) with tissues labeled above each lane. These data are typical of experiments done at least three times with different preparations.

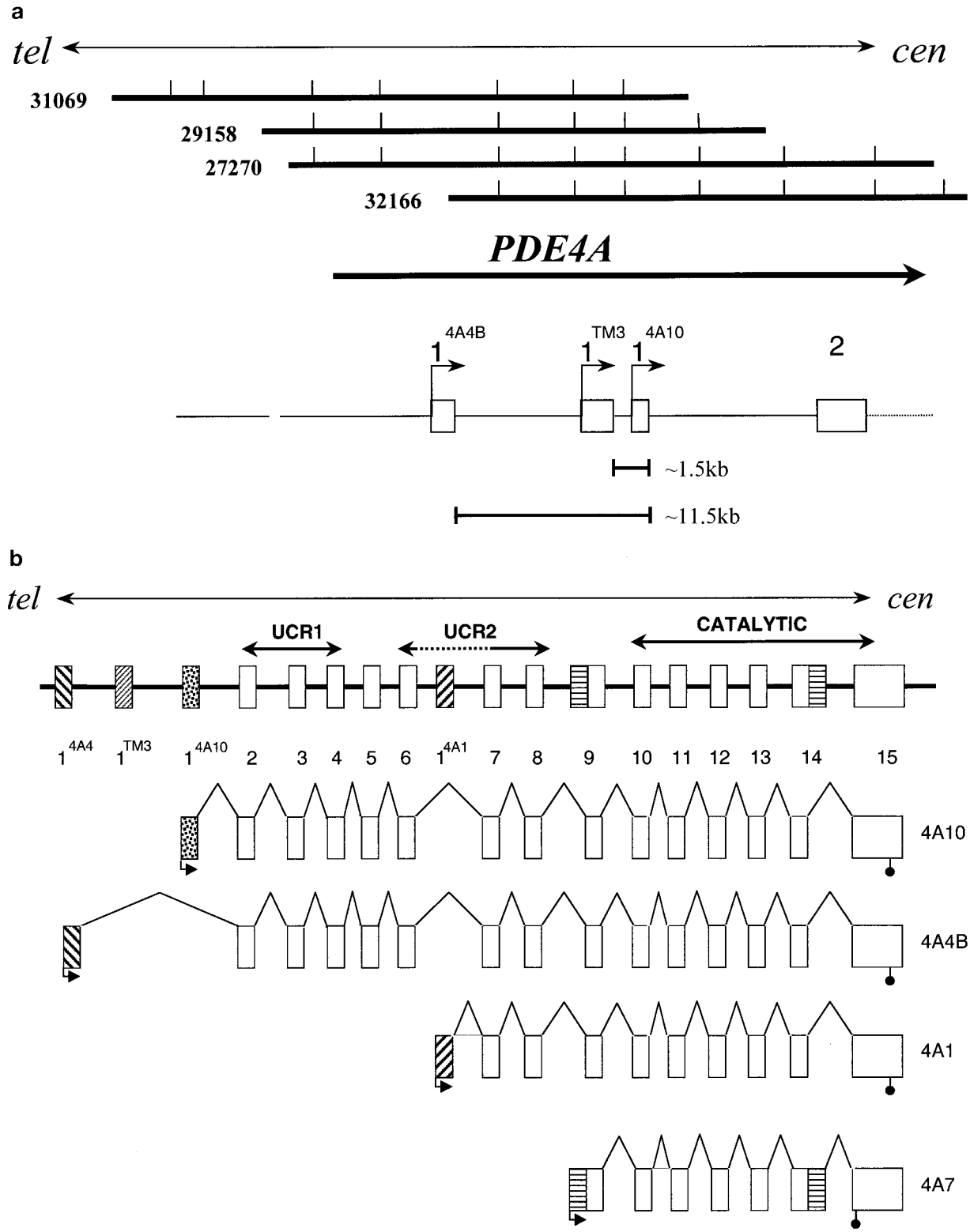

Fig. 4. Location of the PDE4A10 5′ exon on human chromosome 19. a, location of the unique 5′ exon-1^{4A10} on human chromosome 19p13.2 relative to both the unique 5′ exons for the established PDE4A4 long form (exon-1^{4A4}) and the putative TM3 (PDE4A5) long form (exon-1^{TM3}) as well as the first PDE4A common exon, exon-2. Indicated are the positions of the four cosmids, namely, 31069, 29158, 27270, and 32166 that encompass the 5′ end of the contig and contain exon-1^{4A10}. Vertical dashes on the cosmids represent *Eco*RI restriction sites used to map and order cosmids in the contig. The orientation of the PDE4A gene with respect to telomere and centromere is shown at the top. Distances between the extreme 3′ ends of the unique 5′ exons are shown at the bottom. b, exon organization of the human *PDE4A* gene and the splicing that occurs to generate HSPDE4A10 and the other products of this gene found to be conserved across species, namely, the long HSPDE4A4B isoform (pde-46), the supershort HSPDE4A1 (hRD1) isoform, and the catalytically inactive PDE4A7 (2el) isoform. HSPDE4A10 and HSPDE4A4B share 14 exons (2–15) but have unique 5′ exons (exon-1) that encode their unique N-terminal regions. The predicted ORFs in the different variants are marked at the start codon by an arrow and at the termination codon by an anchored circle. The unfilled boxes indicate exons that are common to the various long and short forms while the filled boxes define exons that are unique to particular isoforms.

exon-1^{4A10}. Clone 67 was sequenced and shown to contain all but the final 3′ six nucleotides of the human exon-1^{4A10}. Direct sequencing of cosmid 32166 allowed us to identify the final 6bp of exon-1^{4A10} and its 3′ intron flanking sequence (Fig. 2c).

Comparison of the nucleotide sequence at the 3′ end of exon-1^{4A10} with consensus splice junctions (Mount, 1982) suggests that it represents an authentic splice site (Fig. 2c). Analysis of this genomic sequence also identified an upstream in-frame initiating methionine that would encode, when exon-1^{4A10} was spliced onto the common human PDE4A exons 2 to 15 (Sullivan et al., 1998), an ORF of 825 amino acids, including a unique N terminus of 46 amino acids encoded by exon-1^{4A10} (Figs. 2c and 4b).

We have previously characterized (Sullivan et al., 1998) the positions of the unique first exons that encode the isoform specific N terminus of the established PDE4A4B (pde46) long form and the putative TM3 (HSPDE4A5) long form (Fig. 4). In addition to containing exon-1^{4A10}, we found that exon-1^{TM3} is present in clone 67. Exon-1^{4A10} is situated in proximity to exon-1^{TM3}. Indeed, it is located downstream of exon-1^{TM3} with only 1484 bp separating the extreme 3′ ends of each of the exons (Fig. 4). Thus, exon-1^{4A10} can be located specifically within a defined region of chr19p13.2, downstream of both exon 1^{4A4} and exon 1^{TM3} and 13.5 kb upstream of the common exon 2 (Fig. 4a).

Database Identification of Mouse PDE4A10 cDNA and Genomic Sequence. Using the BLASTN algorithm (Altschul et al., 1990), the expressed sequence tag database, and high throughput genome sequence nucleotide databases (National Center for Biotechnology Information, National Institutes of Health, Bethesda, MD) were queried with the nucleotide sequence that encodes the unique N terminus of the human PDE4A10. One mouse genomic draft sequence (GenBank accession number AC073749) and one mouse EST cDNA (GenBank accession number BE531640) were found to contain sequence that exhibited a high degree of homology with the human PDE4A10 specific 5′ end sequence. Inspection of the murine EST cDNA sequence reveals that 431 bp of unique sequence at the 5′ end are spliced onto the murine *PDE4A* exon-2 (Olsen and Bolger, 2000). The murine EST cDNA sequence exhibited a perfect match with the draft genomic sequence (data not shown) and analysis of the flanking genomic sequence revealed a consensus 5′ splice acceptor site (Mount, 1982) at the same position as that found by us here in the human genomic sequence. Comparison of the human and murine PDE4A10 unique 5′ sequences revealed (Fig. 2a) a conserved initiating methionine residue that predicts an in-frame ORF when spliced onto the common exon-2. It also identifies a high degree of conservation between human and mouse of the isoform-specific N-terminal regions of the murine and human PDE4A10 orthologues (Fig. 2a). Although the human PDE4A10 N terminus consists of 46 amino acids, the murine N terminus contains 45 amino acids. Comparison with the incomplete rat sequence shows that six of the seven residues that differ between human and murine PDE4A10 are completely conserved between mouse and rat with the same amino acid residue, Pro20 (human PDE4A10 residue), deleted (Fig. 2b).

Expression Profile of HSPDE4A10. We set out to assess the distribution of HSPDE4A10 transcripts in various human tissues. A human Rapid-Scan panel was probed using oligonucleotides MS-FB11 and MS-FB12 as a PCR primer pair (Table 1; Fig. 1) to amplify an HSPDE4A10-specific 247-bp fragment. This panel reflected human cDNA prepared from a panel of 22 adult human tissues and two human fetal tissues and was normalized for β-actin. The expected 247-bp product, which was confirmed by sequencing, was evident in a number of tissues (Fig. 3d). The ubiquitously expressed β-actin was equally expressed in all tissues examined (data not shown). This analysis identified HSPDE4A10 transcripts in a large number of distinct tissues. We also used the exon-specific HSPDE4A10 sense primer IM1, together with the PDE4A long isoform, common region, antisense primer ESH4 (Table 1; Fig. 1) to probe a Clontech human panel 1 library of RNA from various human tissues (Fig. 3e). The expected 313-bp product, which was confirmed by sequencing, was evident in a number of organs/tissues. The ubiquitously expressed β-actin was equally expressed in all tissues examined (data not shown).

Similar results were obtained analyzing tissues that were featured in both panels. Of particular note were the strong signals for HSPDE4A10 transcripts in heart and small intestine. Additionally, positive signals were obtained in brain, kidney, spleen, colon, salivary gland, ovary, and peripheral blood lymphocytes. Transcripts were not evident in liver, lung, muscle, stomach, testis, placenta, adrenal glands, pancreas, uterus, prostate, kidney, and bone marrow. Such data indicate that HSPDE4A10 may not be ubiquitously expressed but featured in a defined range of cell types. Interestingly, we did not observe a signal for the presence of HSPDE4A10 transcripts in either fetal brain or liver (Fig. 3d), indicating that the expression of PDE4A10 may be developmentally regulated.

Analysis of the Promoter Activity of the 5′ Region of HSPDE4A10. The 1.34 kb of genomic 5′ flanking sequence lying between the last base of exon-1^{TM3} and the start codon of the human exon-1^{4A10} were analyzed by PROSCAN (version 1.7), a Pol II promoter prediction program (Prestridge, 1995). The PROSCAN program predicted the presence of a promoter between nucleotides −545 and −295 upstream from the start codon of exon-1^{4A10} (Fig. 5a). Although many putative transcription factor binding sites were predicted to be present in this region neither a canonical TATA sequence nor a CAAT box was detected. Similarly, the mouse sequence flanking exon-1^{4A10} lacked both TATA sequence and a CAAT box. The mouse and human 5′ flanking sequences lying upstream of exon-1^{4A10} were compared with each other using the BLAST2 algorithm to identify conserved regions. Two regions that exhibit a high degree of conservation, were found. These were called region A and region B, respectively, (Fig. 5a). Region A contains 90 bp and lies 1077 bp upstream of the human PDE4A10 start codon. Although it lacks any known putative transcription factor binding sites, region A from mouse and human exhibits 77% identity. Region B contains 116 bp and shows 79% identity between mouse and human. This region lies between 401 and 287 bp upstream of the PDE4A10 start codon. The human region B contains several putative transcription factor-binding sites, of these a CREB site and a GC-box are completely conserved in sequence and position in the mouse sequence (Fig. 5c).

We thus set out to determine whether the region found between exon-1^{TM3} and exon-1^{4A10} had promoter-like activity. To do this a 1.8-kb fragment containing 1.67 kb of 5′

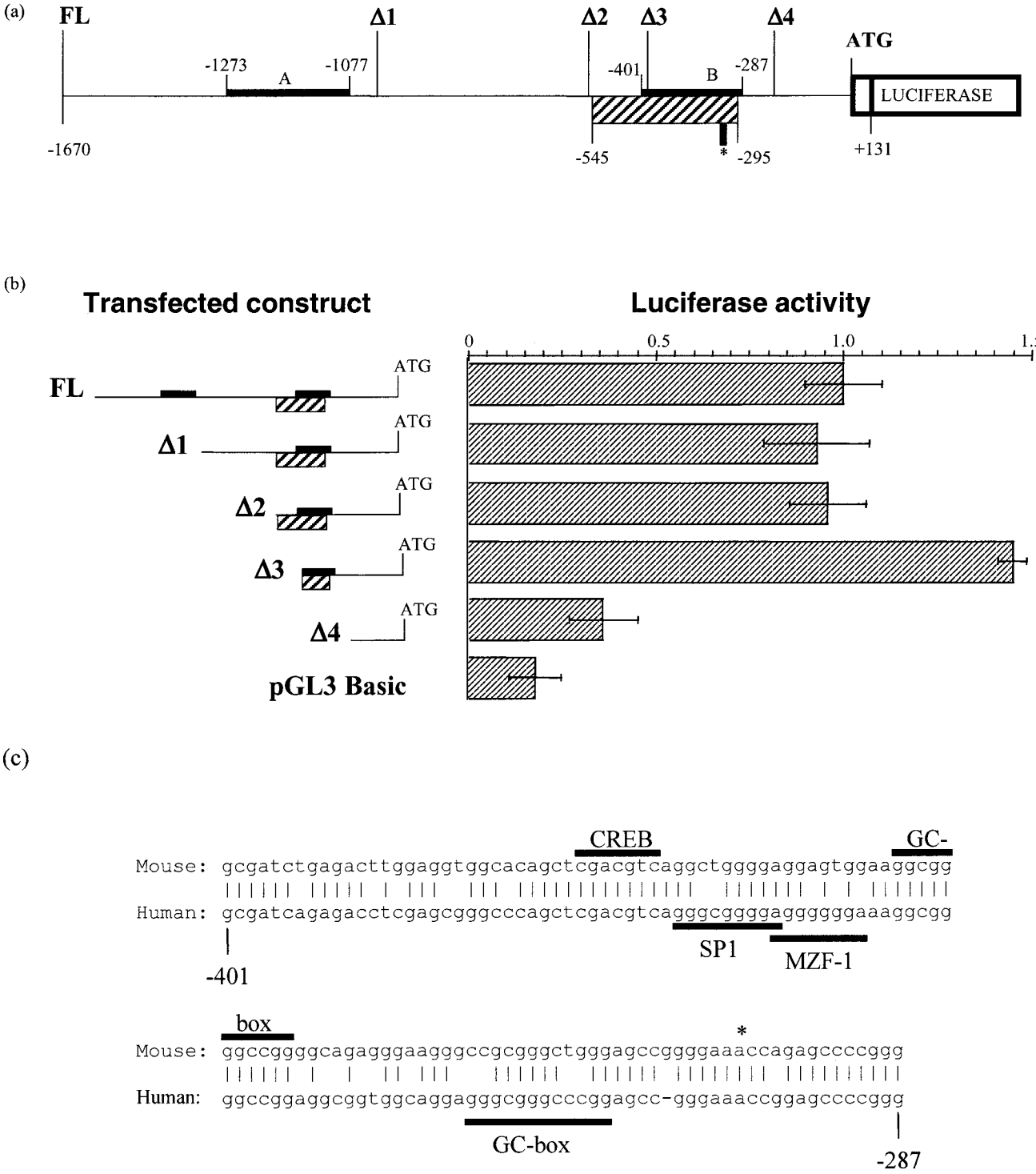

Fig. 5. Promoter analysis of the genomic sequence flanking the 5′ end of the PDE4A10 5′ exon. a, schematic representation of the pFL-Luc construct. Plasmid pFL-Luc contains human genomic sequence from position −1670 to +131 (the start codon of exon-1^{4A10} as base +1) fused in-frame with the luciferase reporter gene in pGL3-basic. The two regions conserved between mouse and human are marked with a thick horizontal line and are labeled A and B with their nucleotide positions marked. The promoter predicted by PROSCAN is shown as a striped box and its nucleotide position is marked. The position of the 5′ deletion point in each of the four deletion constructs are marked and their nucleotide positions are −1049 (Δ1), −548 (Δ2), −389 (Δ3), and −228 (Δ4). b, relative luciferase activity produced after transfection with pGL3-Basic, pFL-Luc, and the four pFL-Luc 5′ deletion constructs Δ1-Δ4 (as shown above). The luciferase activity for pFL-Luc is set to 1 and the activity for the other plasmids is expressed relative to that of pFL-Luc. Luciferase activity is presented as the mean ± S.D. for $n = 4$ separate transfection experiments. c, comparison of mouse and human conserved region B. The mouse genomic sequence (GenBank accession number AC073749) was aligned with its human counterpart using BLAST2. The extreme 5′ base of the mouse PDE4A10 EST (GenBank accession number BE531640) is marked with an asterisk. Position of the human sequence relative to the PDE4A10 start codon is marked below the 5′ and 3′ ends of the sequence. Putative transcription factor-binding sites are marked with horizontal lines above and below the aligned sequences. The binding sites that are completely conserved between human and mouse are marked above the mouse sequence.

flanking sequence was subcloned upstream of the firefly luciferase gene of the pGL3-Basic luciferase reporter vector to generate pFL-Luc. The insert in pFL-Luc thus also contains the first 131 bp of the ORF of PDE4A10, which is fused, in frame, with the firefly luciferase reporter gene (Fig. 5a). The human HEK293 cell line was selected for promoter analysis because we have identified transcripts for PDE4A10 in this cell line (Fig. 3b). Such a region clearly exhibited promoter-like activity in transfected HEK293 cells (Fig. 5b). We were also able to detect activity in transfected SK-N-SH cells that was comparable with that found using HEK293 cells (0.8 ± 0.1 relative light units for pFL-Luc compared with 0.1 ± 0.03 for pGL3-basic alone; mean ± S.D., $n = 4$). However, we were unable to detect any activity in the transfected SMS-SB pre-B-cell line (<6% difference between pFL-Luc and pGL3-basic alone). Thus, it seems likely that such promoter-like activity is cell-type specific.

We noted, however, that serum withdrawal from HEK293 cells, for periods of between 4 and 24 h, caused the promoter-like activity of the pFL-Luc construct to fall by some 38 ± 3% ($n = 6$; mean ± S.D.). The mechanism underpinning such action remains to be determined. However, elevation of cAMP levels with forskolin, IBMX, or both did not alter promoter activity (<10% change) in HEK293 cells. Thus, for unexplained reasons, the CRE locus that is conserved in the human and mouse sequences seems to be inoperative in these cells under these particular conditions. Neither was the activity of pFL-Luc affected by challenge of the transfected HEK293 cells with either phorbol-12-myristate-13-acetate or epidermal growth factor (<10% change).

We wished to determine whether the entire region between the 5′ end of exon-1^{4A10} and the 3′ end of exon-1^{TM3} was required for promoter-like activity. To do this we generated a set of 5′ deletions in pFL-Luc, Δ1-Δ4. The Δ1-pFL-Luc plasmid was chosen to evaluate the effect of the deletion of region A, which exhibits 77% identity in the mouse and human *PDE4A* genes. However, the removal of this region seemed to have little effect on the basal promoter-like activity (Fig. 5b). The Δ2-pFL-Luc plasmid was analyzed because it cuts back to the start of the conserved GC-rich-containing region B that PROSCAN identifies as a putative promoter region. Again, no change in promoter-like activity of this construct was seen (Fig. 5b). The Δ3-pFL-Luc was analyzed because it cuts back to the start of a subregion of region B that is completely conserved in human and mouse (Fig. 5b; heavy line in region B). In this case we observed an increase in promoter-like activity of around 45% (Fig. 5b). The Δ4-pFL-Luc was analyzed because it cuts back before the start of the subregion in region B that is absolutely conserved in human and mouse. This construct, however, had little if any activity over that of the pGL3-Basic luciferase reporter vector (Fig. 5b). This suggests that the 135-bp region found between the Δ3 and Δ4 truncates (Fig. 5a) is important for promoter-like activity.

Localization of HSPDE4A10 in Transiently Transfected COS7 Cells. Two expression constructs, pSV-SPORT4A10 and pSV-SPORT4A10(f2), were generated. Both of these plasmids contain the complete human HSPDE4A10 ORF encoding 825 amino acids. In addition to the HSPDE4A10 ORF, plasmid pSV-SPORT4A10 contains 399 bp of untranslated sequence upstream of the PDE4A10 start codon and includes an upstream out of frame ATG (Fig. 2b). The construct pSV-SPORT4A10(f2) was generated to remove the 5′-untranslated sequence, including the upstream out of frame ATG, which has the potential to lower the efficiency of translation of the PDE4A10 ORF.

The pSV-SPORT4A10(f2)-transfected COS7 cells exhibited a PDE activity of 3 to 5 nmol/min/mg protein compared with 3 to 6 pmol/min/mg protein for the untransfected cells (range; $n = 3$). Over 98% of the PDE activity in these transfected cells could be inhibited by the PDE4 selective inhibitor rolipram (10 μM) using 1 μM cAMP as substrate. This indicates that the recombinant activity was indeed that of a rolipram-inhibited PDE4 enzyme. Similar results were obtained for the pSV-SPORT4A10 transfected COS7 cells, which exhibited a specific activity of 4 to 6 pmol/min/mg protein.

COS7 cells transfected with these plasmids were subjected to immunoblotting using a human PDE4A-specific antiserum (Huston et al., 1996). This detects the C-terminal region found in common to all active PDE4A isoforms. Transfection with either plasmid allowed us to detect a single immunoreactive species that comigrated upon SDS-PAGE (Fig. 6a). These had molecular sizes of 120.9 ± 1.0 and 120.7 ± 0.7 for expression determined by pSV-SPORT4A10 and pSV-SPORT4A10(f2), respectively ($n = 3$; mean ± S.D.). This indicates that the single in-frame methionine identified at the start of exon-1^{4A10} does indeed serve as a functional initiator of translation.

COS7 cells that had been transfected with pSV-SPORT4A10(f2) were subjected to fractionation to isolate a high-speed supernatant soluble (S2) fraction, together with high-speed pellet (P2) and low-speed pellet (P1) fractions. Quantitative ELISA and immunoblotting analyses showed that HSPDE4A10 was predominantly localized in the S2 fraction (Table 2). Similar results were obtained after the distribution of HSPDE4A10 activity (1 μM cAMP substrate) with 83 ± 8% in the S2 fraction, 4 ± 2% in P2, and 13 ± 6% in P1 fractions (means ± S.D.; $n = 3$). This distribution was, however, markedly different from that seen in COS7 cells transfected to express HSPDE4A4B (Table 2) and as reported previously (McPhee et al. 1999).

We also treated these various fractions with a range of concentrations (0.025–1%; identical protein concentrations) of the nonionic detergent Triton X-100 and determined PDE activity. All fractions gave an identical response (data not shown), namely, a fall in activity of 18 ± 5% (mean; $n = 3$ experiments).

Analysis by laser-scanning confocal microscopy showed that HSPDE4A10 was highly localized to the perinuclear region of transfected COS cells (Fig. 5c), with little found near the cell margin. This indicates that the major fraction of HSPDE4A10 may well be associated with subcellular structures in intact COS cells. That this was not evident subsequent to subcellular fractionation indicates that particulate association is critically dependent upon cell integrity. For example, if the level of expression of PDE4A10 were to allow it to associate with a low-affinity anchor, then one would expect this to be lost upon dilution consequent to cell disruption. Similarly, if association were dependent upon cell energy status then, again, dissociation would ensue upon cell disruption.

Pull-down (sedimentation) assays have been used to show that the SH3 domain of LYN tyrosyl kinase, expressed as a GST fusion protein, binds to the long HSPDE4A4B isoform. Deletion analyses then showed that the unique N terminus of

this isoform provided the major site of interaction with LR2 providing another site of interaction (McPhee et al., 1999). Here we show that although HSPDE4A10 can also interact with the SH3 domain of LYN, it does so only weakly compared with HSPDE4A4B (Fig. 6d). The degree of interaction seems to be similar to that seen using an N-terminally truncated PDE4A species (h61; HSPDE4A4C) that represents the core PDE4A region found in all long PDE4A isoforms (Fig. 6d). Using equal amounts of these various HSPDE4A species in pull-down assays we were able to show that the binding of HSPDE4A10 and h6.1 to LYN-SH3 was 28 ± 6 and 30 ± 5%, respectively, of that seen using HSPDE4A4B (mean ± S.D.; conditions as described under *Materials and Methods*). We have shown previously (McPhee et al., 1999) for h6.1 that deletion of the proline- and arginine-rich sequence within LR2, as in the Δb-h6.1 mutant, led to loss of interaction with LYN-SH3. Similarly, we show here that the cognate Δb-HSPDE4A10 construct failed to interact with LYN-SH3 (Fig. 6d).

Properties of HSPDE4A10 Expressed in COS7 Cells. Kinetic evaluation was done on HSPDE4A10 activity found in both the soluble (S2) and particulate (P1, P2) fractions of transfected COS7 cells. These showed that the HSPDE4A10 activity in the various fractions exhibited very similar K_m values (Table 2). In an attempt to determine whether the relative V_{max} values for HSPDE4A10 expressed in these various fractions was different, we assessed the relative amount of HSPDE4A10 protein in each fraction immunologically using both an ELISA assay and, to similar effect, by quantitative immunoblotting. We then determined PDE activities using equal amounts of immunoreactive HSPDE4A10 in the assays. Through this procedure we were able to gauge the relative V_{max} values for the enzymes in the three different subcellular fractions. These are given with respect to the activity in the S2 fraction expressed as unity (Table 2). It was evident from such studies that the particulate form of HSPDE4A10 was considerably less active than the soluble form found in the S2 fraction.

We took equal amounts (2 μg) of protein from P2 and S2 fractions of COS7 cells that had been transfected to expressed HSPDE4A10 and determined the PDE activity in each of these fractions (1 μM cAMP) separately and also when they were mixed together. On the basis of simple additivity, one would expect to obtain a value of unity for the ratio of the experimentally determined activity of this mixture over the calculated sum of the activities measured in each of the individual fractions. However, we obtained a value of 0.57 ± 0.10 (mean; $n = 3$ separate experiments), which was considerably less than expected. One possibility is that soluble HSPDE4A10 might interact with a component in

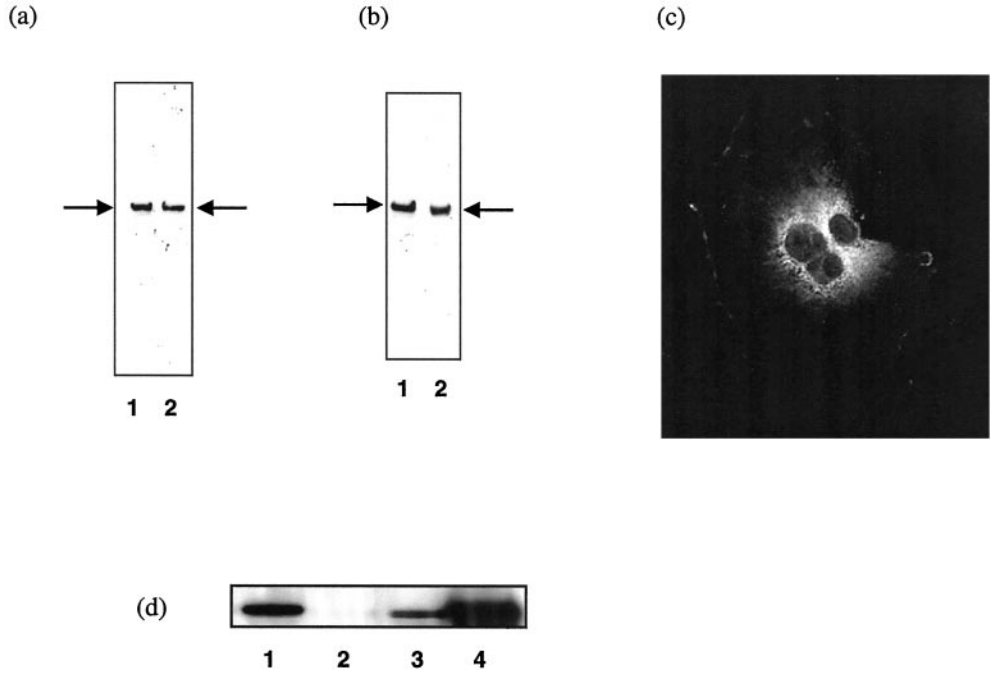

Fig. 6. Expression of HSPDE4A10 in COS7 cells. a, COS7 cells were transfected with either a plasmid, pSV. SPORT4A10 (track 1), containing the entire PDE4A10 ORF together with 399 bp of untranslated sequence upstream of the PDE4A10 start codon, or the plasmid pSV. SPORT4A10(f2) (track 2) where this 5′ untranslated region was removed (under *Materials and Methods*). These transfected cells were then analyzed by SDS-PAGE with subsequent immunoblotting using an antisera specific for the common C-terminal region of human PDE4A isoforms (Huston et al., 1996). In both instances a single, comigrating PDE4A immunoreactive species of 121 kDa was observed. b, COS7 cells were transfected with either a plasmid expressing PDE4A4B (track 1) or pSV. SPORT4A10(f2) (track 2) and then analyzed by SDS-PAGE with subsequent immunoblotting using an antisera specific for the common C-terminal region of human PDE4A isoforms (Huston et al., 1996). In both instances a single immunoreactive species was observed, this being of 121 kDa for PDE4A10 and 1245 kDa for PDE4A4B (pde46). c, COS7 cells were transfected to express PDE4A10 and then fixed and treated so as to immunolocalize this enzyme as described under *Materials and Methods*. This shows a section through the center of a typical transfected cell as imaged using laser-scanning confocal analysis. The focus of fluorescent material was in the perinuclear region of the cell. d, result of a typical pull-down assay performed using a GST fusion protein of the LYN kinase SH3 domain, as described under *Materials and Methods*. Identification of associated PDE4A species was achieved by immunoblotting, using a PDE4A specific antiserum, equal amounts of each of the harvested glutathionine agarose beads. In each instance, GST-LYN-SH3 bound to glutathionine agarose was first incubated with equal immunoreactive amounts of the indicated PDE4A species from the soluble (S2) fraction of transfected COS7 cells. Shown are pull-downs using the truncate h6.1 (HSPDE4A4C) (track 1), Δb-PDE4A10 (track 2), PDE4A410 (track 3), and PDE4A4B (track 4). No binding was observed using GST bound to glutathionine agarose (data not shown). These data are typical of experiments done at least three times with different preparations.

the P2 fraction such as to reduce its activity to the level seen comparing isolated PDE4A10 activity in the P2 and S2 fractions (Table 2). Making the assumption that the activity of the entire S2 pool could be so diminished, then one can recalculate the above-mentioned ratio after adjustment of the S2 activity to such a predicted lower activity level. Doing this yielded a value of near unity (1.1). It is possible, therefore, that in mixing these subcellular fractions, at least a proportion of the activity of soluble HSPDE4A10 from the S2 fraction was reduced in activity, probably through its interaction with a component in the P2 fraction.

We used both quantitative ELISA and immunoblotting approaches to evaluate whether the maximum activity of HSPDE4A10 differed from that of HSPDE4A4B. Thus, we determined the activities of equal immunoreactive amounts of each of these proteins expressed in the S2 fraction of transfected COS7 cells. In doing this, we found no discernible difference (<8%; $n = 3$ separate experiments) between the maximal activities of HSPDE4A10 and HSPDE4A4B.

We determined the IC_{50} values for inhibition of HSPDE4A10 activity by rolipram (Fig. 7; Table 2). The forms of HSPDE4A10 found in the various subcellular fractions proved to be similarly sensitive to inhibition by rolipram (Table 1). The IC_{50} values for inhibition by rolipram of Δb-PDE4A10 expressed in the P2 and S2 fractions were also very similar, being 51 ± 10 and 46 ± 8 nM (mean ± S.D.; $n = 3$; [cAMP] = 1 μM).

Conformationally distinct forms of proteins can exhibit distinct sensitivities to thermal denaturation. In the case of enzymes this can be monitored by following the loss of catalytic activity over time of incubation at a denaturing temperature. Here, then we showed (Fig. 7) that particulate-associated HSPDE4A10 was considerably more thermolabile than its soluble form, with half-lives for decay of activity of 5.0 ± 0.3 and 11.2 ± 1.2 min for HSPDE4A10 activity in the P2 and S2 fractions, respectively (means ± S.D., $n = 3$ separate experiments).

In addition to this, we found that the activity of HSPDE4A4B was considerably more thermostable than that of HSPDE4A10 (Fig. 7). We thus observed $T_{0.5}$ values of 12.5 ± 0.9 and 22.3 ± 1.8 min for HSPDE4A4B activity in the P2 and S2 fractions, respectively (means ± S.D., $n = 3$ separate experiments). The thermostability of both these PDE4A isoforms present in the P1 fraction of transfected COS7 cells was very similar to that of the P2-expressed forms, with $T_{0.5}$ of 5.8 ± 0.6 and 11.7 ± 1.1 min for HSPDE4A10 and HSPDE4A4B, respectively (mean ± S.D.; $n = 3$).

Discussion

Here, we have identified a novel PDE4A isoform, called PDE4A10, that is conserved in human, rat, and mouse. Like all known, catalytically active, PDE4A isoforms, PDE4A10 is defined by its unique N-terminal region. PDE4A10 represents a novel long form PDE4A isoform with the human HSPDE4A10 ORF encoding an 825 amino acid enzyme. RT-PCR screens, to detect transcripts, indicated that

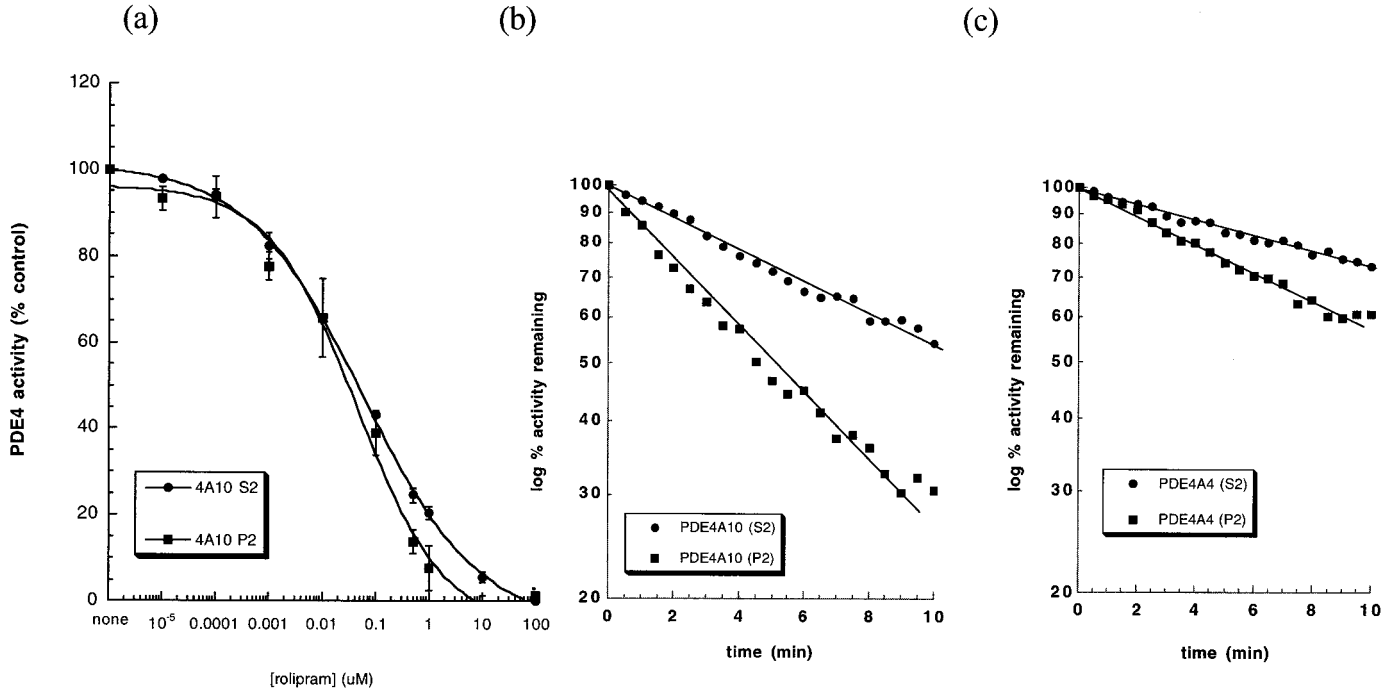

Fig. 7. Analysis of the activity of PDE4A10 expressed in COS7 cells. a, COS7 cells were transfected with pSV. SPORT4A10(f2), harvested, lysed, and the high-speed particulate (P2) and supernatant (S2) fractions prepared as described under *Materials and Methods*. The sensitivity of PDE4 activity in these fractions to inhibition by rolipram was then analyzed at a cAMP concentration that was equal to the K_m concentration (Table 2). To allow ready comparison, we have plotted the PDE activity as a percentage of that observed in the untreated control enzyme in each of the indicated fractions. Data shown are the means of three separate experiments done on different cell transfections with errors as SD. COS7 cells were transfected so as to express either PDE4A10 [pSV. SPORT4A10(f2)] (b) or PDE4A4B (c), harvested, lysed, and particulate (P2) and high-speed supernatant, soluble (S2) fractions prepared as described under *Materials and Methods*. The sensitivity of the PDE activity of these two enzymes to thermal inactivation at 55°C is shown. Thermal inactivation of a single species is a first order process and thus its decay follows a single exponential. As such, plots of log % activity remaining will be linear and can be used to derive half-lives. Data are the means of analyses done on three separate occasions using different transfections of COS7 cells.

HSPDE4A10 is not ubiquitously expressed but is likely to be found in a specific range of cell types.

As with all PDE4 enzymes analyzed to date (Houslay et al., 1998), PDE4A10 migrated with an apparent size (121 kDa) that was greater than that which could be predicted on the basis of primary sequence data alone, namely, 91 kDa. This observation compares with a molecular size of 125 kDa observed for immunoblotting of the long PDE4A4B isoform (Fig. 5b; Huston et al., 1996) whose predicted size is 98 kDa (Houslay et al., 1998). It should be noted, however, that the similarity in size of both PDE4A4B and PDE4A10 (Fig. 5b) offers considerable potential for confusing the identity of these enzymes in analyses involving SDS-PAGE. Indeed, this is likely to be exacerbated in situations where both of these PDE4A species are present.

The unique N terminus of HSPDE4A10 is 46 amino acids long and is highly conserved in mouse and rat, indicating conservation of function. Indeed it, seemingly, confers novel properties on HSPDE4A10 as indicated by comparative analyses with the established HSPDE4A4B long form. These differences include sensitivity to inhibition by the PDE4-selective inhibitor rolipram, intracellular distribution, and thermostability. Thus, soluble HSPDE4A10, found in the S2 fraction, is exquisitely sensitive to inhibition by rolipram (IC_{50} = 56 nM) compared with HSPDE4A4B (IC_{50} = 1250 nM; Huston et al., 1996; Houslay et al., 1998). This suggests that processes governed by their N-terminal regions affects the conformation of the catalytic unit of these enzymes. Indeed, we show here that, expressed in the S2 fraction, HSPDE4A10 is considerably more thermolabile than HSPDE4A4B. This is consistent with the catalytic unit of these two long PDE4A isoforms adopting different conformations.

Interestingly, the particulate-associated forms of both HSPDE4A10 and HSPDE4A4B showed decreased thermostability compared with the S2, soluble forms. Thus, particulate-association would also seem to trigger either directly or indirectly a conformational change in the catalytic site of both of these isoforms. This may underpin our observation that the particulate-located forms of both HSPDE4A10 and HSPDE4A4B exhibited lowered maximal catalytic activities compared with their S2-located, soluble forms (Table 2; Huston et al., 1996). Furthermore, in the case of HSPDE4A4B, association with particulate fractions dramatically increased its sensitivity to inhibition by rolipram (IC_{50} = 120 nM; Huston et al., 1996; McPhee et al., 1999). This was not seen with HSPDE4A10, either because its catalytic unit has already adopted a "high-affinity" rolipram-inhibited status (Souness et al., 1997; Houslay et al., 1998; Torphy, 1998) or because, unlike HSPDE4A4B (McPhee et al., 1999), it does not interact as strongly with SH3 domain-containing proteins. SH3 domain-interaction with HSPDE4A4B is mediated, primarily, by PXXPXXR sites within its unique N-terminal region together with a site located within LR2 (Fig. 1). However, the "switching" of HSPDE4A4B to a high-affinity rolipram-inhibited state can be ablated by deletion of a proline- and arginine-rich region, within LR2, as shown in the Δb-HSPDE4A4B mutant (McPhee et al., 1999). We show here, however, that generation of the cognate mutant in HSPDE4A10 failed to alter its sensitivity to inhibition rolipram, thus further emphasizing the difference in the properties of these two long PDE4A isoforms.

Laser-scanning confocal immunofluorescence analyses imply that both HSPDE4A4B (Huston et al., 1996; McPhee et al., 1999) and HSPDE4A10 (this study) may be predominantly particulate-associated in intact cells. Nevertheless, soluble forms of both of these enzymes are released upon cellular disruption. This may be indicative of the reversible association of these PDE4A isoforms with certain intracellular anchor sites, where either dilution, consequent to disruption, or cell disruption per se serves to liberate certain particulate-associated component. Such interactions seem to be very different for these two isoforms because cell disruption released about 83% of HSPDE4A10 into the S2 fraction, whereas only around 58% of HSPDE4A4B was released (Table 2). These data suggest that their unique N-terminal regions are likely to play a role in the different intracellular targeting of these isoforms. Thus, HSPDE4A10 exhibited a predominantly perinuclear localization (Fig. 6c), whereas HSPDE4A4B was found associated with the cortical cytoskeleton, including lamellae, pseudopods, and ruffles at the cell margin, as well as to structures throughout the cell body (Huston et al., 1996; McPhee et al., 1999). Certainly, the intracellular localization of HSPDE4A4B, expressed in COS7 cells has been shown to be influenced by the ability of its N-terminal region to interact with the SH3 domain of the tyrosyl kinase LYN (Huston et al., 1996). Indeed, we have recently demonstrated (Huston et al., 2000) that RNPDE4A5, the rat orthologue of HSPDE4A4B, showed a remarkable intracellular redistribution in intact cells subsequent to the caspase-3 performed cleavage of the portion of its unique N-terminal region that confers SH3-domain interaction. This would be consistent with the notion that the SH3-interacting region of PDE4A4B plays a role in its intracellular targeting (Huston et al., 1996; McPhee et al., 1999).

The human genomic 5′ flanking sequence, located upstream from exon-1^{4A10}, lacks both a TATA sequence and CAAT box but does contain a predicted pol-II promoter in the region −545 to −295 bp upstream of the PDE4A10 start codon (Fig. 5). Incorporation of this region into a luciferase reporter construct (pFL-Luc) and transfection into HEK293 cells allowed us to demonstrate that it did indeed have promoter-like activity. That we also identified such activity upon transfection of SK-N-SH cells but not of the SMS-SB pre-B-cell line indicates that the functioning of this promoter-like activity may be cell-type specific. This would be consistent with our finding that transcripts for HSPDE4A10 are not ubiquitously expressed.

Comparison of the mouse and human genomic sequences located upstream of the respective species' exon-1^{4A10} identified two conserved regions, called here region A and B, which we have explored using by generating a set of deletion constructs of pFL-Luc (Fig. 5). Thus, removal of the conserved region A and sequence up to the predicted promoter region had little effect on the promoter activity in HEK293 cells (Fig. 5). In contrast to this, removal of the first 156 bp of the predicted promoter region and the first 12 bp of conserved region B resulted in a 50% increase in promoter activity. The increase in promoter activity of Δ3-pFL-Luc suggests that sequences between −548 and −389 may bind factors that inhibit promoter activity in HEK293 cells. Further deletion to remove all of the predicted promoter and conserved region B (Δ4-pFL-Luc) resulted in loss of promoter activity. The core promoter region lying between positions −389 and −228

contains all but 12 bp of region B that is conserved between human and mouse (Fig. 5). The human region B contains a number of putative transcription factor binding sites with the CREB and GC-box recognition sequences being completely conserved between the two species (Fig. 5c). This core region also contains putative SP1 sites, is 78% GC-rich overall, and contains two putative sites for the myeloid-enriched transcription factor MZF1 whose presence has been shown to regulate basal transcription in TATA-less promoters (Kida et al., 1999). It also contains multiple potential CAP sites of which one is evident within the minimal region (data not shown). This 5′ flanking sequence, located upstream from exon-1^{4A10}, also exhibits putative binding sites (data not shown) for a variety of transcription factors associated with myeloid cell differentiation and the functioning of hematopoietic cells. Indeed, promoters associated with myeloid differentiation invariably lack a TATA box or defined initiation sequence (Tenen et al., 1997). Of potential interest are putative sites for GATA, which has been shown to interact with MZF1 (Kida et al., 1999) and also the H_2O_2-activated USF (Andrews, 2000) as well as CREB and nuclear factor-κB. This might suggest an important role for PDE4A10 in the inflammatory response. Certainly that would be in accord with the established role of PDE4 inhibitors in attenuating inflammatory processes (Schudt et al., 1995; Torphy, 1998; Giembycz, 2000). These various features are consistent with this 5′ flanking region expressing promoter-like activity. However, it is clear that further work is required to appreciate the subtleties of regulation of this isoform in different cell backgrounds. Indeed, little at all is known about the promoters that control the expression of members of any of the multigene PDE family. However, there is evidence that a promoter that lacks both TATA and CAAT boxes serves to control the expression of rodent PDE4D short forms (Vicini and Conti, 1997). This rodent PDE4D short form promoter, as with that for HSPDE4A10, contains SP1 sites and GC-rich regions that often characterize the growing number of promoters shown to lack a TATA box (Bucher, 1990; Clegg et al., 1996; Tenen et al., 1997).

The unique N-terminal regions of HSPDE4A10 and HSPDE4A4B seem to play a key role in regulating the conformation of the enzyme catalytic unit and influencing intracellular localization. Indeed, there is currently much interest in the notion that the distinct intracellular localization of particular PDE4 isoforms may contribute to their functional role in cells (Houslay and Milligan, 1997; Houslay et al., 1998). This may allow such isoforms to regulate signaling in functionally distinct "pools" of cAMP (Klauck and Scott, 1995; Houslay and Milligan, 1997; Houslay et al., 1998; Colledge and Scott, 1999). Thus, the development of methods of inactivating specific PDE4 isoforms may prove to be of therapeutic significance. To begin to achieve this, it is crucial to identify the full range of human PDE4 isoforms and their expression patterns.

References

Altschul SF, Gish W, Miller W, Myers EW and Lipman DJ (1990) Basic local alignment search tool. *J Mol Biol* **215:**403–410.

Andrews GK (2000) Regulation of metallothionein gene expression by oxidative stress and metal ions. *Biochem Pharmacol* **59:**95–104.

Beard MB, Olsen AE, Jones RE, Erdogan S, Houslay MD and Bolger GB (2000) UCR1 and UCR2 domains unique to the cAMP-specific phosphodiesterase (PDE4) family form a discrete module via electrostatic interactions. *J Biol Chem* **275:** 10349–10358.

Beavo JA (1995) Cyclic nucleotide phosphodiesterases: functional implications of multiple isoforms. *Physiol Rev* **75:**725–748.

Bolger G (1994) Molecular Biology of the cyclic AMP-specific cyclic nucleotide phosphodiesterases: a diverse family of regulatory enzymes. *Cell Signal* **6:**851–859.

Bolger GB, McPhee I and Houslay MD (1996) Alternative splicing of cAMP-specific phosphodiesterase mRNA transcripts. Characterization of a novel tissue-specific isoform, RNPDE4A8. *J Biol Chem* **271:**1065–1071.

Bolger G, T Michaeli, T Martins, T St John, B Steiner, L Rodgers, M Riggs, M Wigler and K Ferguson (1993) A family of human phosphodiesterases homologous to the dunce learning and memory gene product of *Drosophila melanogaster* are potential targets for antidepressant drugs. *Mol Cell Biol* **13:**6558–6571.

Bolger GB, Rodgers L and Riggs M (1994) Differential CNS expression of alternative mRNA isoforms of the mammalian genes encoding cAMP-specific phosphodiesterases. *Gene* **149:**237–244.

Bucher P (1990) Weight matrix descriptions of four eukaryotic RNA polymerase II promoter elements derived from 502 unrelated promoter sequences. *J Mol Biol* **212:**563–578.

Clegg CH, Haugen HS and Boring LF (1996) Promoter sequences in the RI beta subunit gene of cAMP-dependent protein kinase required for transgene expression in mouse brain. *J Biol Chem* **271:**1638–1644.

Colledge M and Scott JD (1999) AKAPs: from structure to function. *Trends Cell Biol* **9:**216–221.

Conti M and Jin SLC (1999) The molecular biology of cyclic nucleotide phosphodiesterases. *Prog Nucleic Acid Res* **63:**1–38.

Davis RL, Takayasu H, Eberwine M and Myres J (1989) Cloning and characterisation of mammalian homologs of the *Drosophila* dunce+ gene. *Proc Natl Acad Sci USA* **86:**3604–3608.

Giembycz MA (2000) Phosphodiesterase 4 inhibitors and the treatment of asthma: where are we now and where do we go from here? *Drugs* **59:**193–212.

Horton YM, Sullivan M and Houslay MD (1995) Molecular cloning of a novel splice variant of human type IV(A) (PDE- IV(A)) cyclic AMP phosphodiesterase and localization of the gene to the p13.1-q12 region of human chromosome 19. *Biochem J* **308:**683–691.

Houslay MD and Milligan G (1997) Tailoring cAMP signalling responses through isoform multiplicity. *Trends Biochem Sci* **22:**217–224.

Houslay MD, Sullivan M and Bolger GB (1998) The multi-enzyme PDE4 cyclic AMP specific phosphodiesterase family: intracellular targeting, regulation and selective inhibition by compounds exerting anti-inflammatory and anti-depressant actions. *Adv Pharmacol* **44:**225–242.

Huston E, Beard M, McCallum F, Pyne NJ, Vandenabeele P, Scotland G and Houslay MD (2000) The cAMP-specific phosphodiesterase PDE4A5 is cleaved downstream of its SH3 interaction domain by caspase-3: consequences for altered intracellular distribution. *J Biol Chem* **275:**28063–28074.

Huston E, Lumb S, Russell A, Catterall C, Ross AH, Steele MR, Bolger GB, Perry M, Owens R and Houslay MD (1997) Molecular cloning and transient expression in COS7 cells of a novel human PDE4B cyclic AMP specific phosphodiesterase, HSPDE4B3. *Biochem J* **328:**549–558.

Huston E, Pooley L, Julien J, Scotland Julien, McPhee I, Sullivan M, Bolger G and Houslay MD (1996) The human cyclic AMP-specific phosphodiesterase PDE-46 (HSPDE4A4B) expressed in transfected COS7 cells occurs as both particulate and cytosolic species which exhibit distinct kinetics of inhibition by the anti-depressant rolipram. *J Biol Chem* **271:**31334–31344.

Kida M, Souri M, Yamamoto M, Saito H and Ichinose A (1999) Transcriptional regulation of cell type-specific expression of the TATA- less A subunit gene for human coagulation factor XIII. *J Biol Chem* **274:**6138–6147.

Klauck TM and Scott JD (1995) The postsynaptic density: a subcellular anchor for signal transduction enzymes. *Cell Signal* **7:**747–757.

Livi GP, Kmetz P, McHale MM, Cieslinski LB, Sathe GM, Taylor DP, Davis RL, Torphy TJ and Balcarek JM (1990) Cloning and expression of cDNA for a human low-K(m), rolipram-sensitive cyclic AMP phosphodiesterase. *Mol Cell Biol* **10:** 2678–2686.

MacKenzie SJ and Houslay MD (2000) The action of rolipram on specific PDE4 cAMP phosphodiesterase isoforms and on the phosphorylation of CREB and p38 MAP kinase in U937 monocytic cells. *Biochem J* **347:**571–578.

Manganiello VC, Murata T, Taira M, Belfrage P and Degerman E (1995a) Diversity in cyclic nucleotide phosphodiesterase isoenzyme families. *Arch Biochem Biophys* **322:**1–13.

Manganiello VC, Taira M, Degerman E and Belfrage P (1995b) Type III cGMP-inhibited cyclic nucleotide phosphodiesterases (PDE 3 gene family). *Cell Signal* **7:**445–455.

Marchmont RJ and Houslay MD (1980) An intrinsic and a peripheral protein constitute the cyclic AMP phosphodiesterase activity of rat liver plasma membranes. *Biochem J* **187:**381–392.

McPhee I, Pooley L, Lobban M, Bolger G and Houslay MD (1995) Identification, characterization and regional distribution in brain of RPDE-6 (RNPDE4A5), a novel splice variant of the PDE4A cyclic AMP phosphodiesterase family. *Biochem J* **310:**965–974.

McPhee I, Yarwood SJ, Huston E, Scotland Huston, Beard MB, Ross AH, Houslay ES and Houslay MD (1999) Association with the src family tyrosyl kinase lyn triggers a conformational change in the catalytic region of human cAMP-specific phosphodiesterase HSPDE4A4B: consequences for rolipram inhibition. *J Biol Chem* **274:** 11796–11810.

Mount SM (1982) A catalogue of splice junction sequences. *Nucleic Acids Res* **10:** 459–472.

O'Connell JC, McCallum JF, McPhee I, Wakefield J, Houslay ES, Wishart W, Bolger G, Frame M and Houslay MD (1996) The SH3 domain of Src tyrosyl protein kinase interacts with the N-terminal splice region of the PDE4A cyclic AMP specific phosphodiesterase RPDE-6 (RNPDE4A5). *Biochem J* **318:**255–262.

Olsen AE and Bolger GB (2000) Physical mapping and promoter structure of the murine cAMP-specific phosphodiesterase pde4a gene. *Mamm Genome* **11:**41–45.

Prestridge DS (1995) Predicting Pol II promoter sequences using transcription factor binding sites. *J Mol Biol* **249:**923–932.
Rena G and Houslay MD (1998) A simple method for sequencing small DNAs by introducing precise overlapping ends into restriction digestion fragments. *Nucleic Acids Res* **26:**3867–3868.
Rogers DF and Giembycz MA (1998) Asthma therapy for the 21st century. *Trends Pharmacol Sci* **19:**160–164.
Schudt C, Tenor H and Hatzelmann A (1995) PDE isoenzymes as targets for anti-asthma drugs. *Eur Respir J* **8:**1179–1183.
Seybold J, Newton R, Wright L, Finney Wright, Suttorp N, Barnes PJ, Adcock IM and Giembycz MA (1998) Induction of phosphodiesterases 3B, 4A4,4D1, 4D2, and 4D3 in Jurkat T-cells and in human peripheral blood T-lymphocytes by 8-bromo-cAMP and Gs-coupled receptor agonists. Potential role in beta2-adrenoreceptor desensitization. *J Biol Chem* **273:**20575–20588.
Shakur Y, Pryde JG and Houslay MD (1993) Engineered deletion of the unique N-terminal domain of the cyclic AMP-specific phosphodiesterase RD1 prevents plasma membrane association and the attainment of enhanced thermostability without altering its sensitivity to inhibition by rolipram. *Biochem J* **292:**677–686.
Shakur Y, Wilson M, Pooley L, Lobban M, Griffiths SL, Campbell AM, Beattie J, Daly C and Houslay MD (1995) Identification and characterization of the type-IVA cyclic AMP-specific phosphodiesterase RD1 as a membrane-bound protein expressed in cerebellum. *Biochem J* **306:**801–809.
Souness JE and Rao S (1997) Proposal for pharmacologically distinct conformers of PDE4. *Cell Signal* **9:**227–236.
Sullivan M, Rena G, Begg F, Gordon L, Olsen AS and Houslay MD (1998) Identification and characterization of the human homologue of the short PDE4A cAMP-specific phosphodiesterase RD1 (PDE4A1) by analysis of the human HSPDE4A gene locus located at chromosome 19p13.2. *Biochem J* **333:**693–703.
Tenen DG, Hromas R, Licht JD and Zhang DE (1997) Transcription factors, normal myeloid development, and leukemia. *Blood* **90:**489–519.
Thompson WJ and Appleman MM (1971) Multiple cyclic nucleotide phosphodiesterase activities from rat brain. *Biochemistry* **10:**311–316.
Torphy TJ (1998) Phosphodiesterase isozymes: molecular targets for novel anti-asthma agents. *Am J Respir Crit Care Med* **157:**351–370.
Torphy TJ, Barnette MS, Underwood DC, Griswold Underwood, Christensen SB, Murdoch RD, Nieman RB and Compton CH (1999) Ariflo (SB 207499), a second generation phosphodiesterase 4 inhibitor for the treatment of asthma and COPD: from concept to clinic. *Pulm Pharmacol Ther* **12:**131–135.
Vicini E and Conti M (1997) Characterization of an intronic promoter of a cyclic adenosine 3′,5′-monophosphate (cAMP)-specific phosphodiesterase gene that confers hormone and cAMP inducibility. *Mol Endocrinol* **11:**839–850.
Yarwood SJ, Steele MR, Scotland G, Houslay MD and Bolger GB (1999) The RACK1 signaling scaffold protein selectively interacts with the cAMP-specific phosphodiesterase PDE4D5 isoform. *J Biol Chem* **274:**14909–14917.

Send reprint requests to: Prof. Miles Houslay, Molecular Pharmacology Group, Division of Biochemistry and Molecular Biology, Davidson Building, Institute of Biomedical and Life Sciences, University of Glasgow, Glasgow G12 8QQ, Scotland, UK. E-mail: m.houslay@bio.gla.ac.uk